τ neutrinos in KM3NeT

THESIS

submitted in partial fulfillment of the
requirements for the degree of

MASTER OF SCIENCE
in
PHYSICS

Author :	Freek Broeren
Student ID :	0910651
Supervisor :	Dr. D.F.E. Samtleben
2^{nd} corrector :	Dr.Ir. S.J. van der Molen

Leiden, The Netherlands, December 15, 2015

τ neutrinos in KM3NeT

Freek Broeren

Huygens-Kamerlingh Onnes Laboratory, Leiden University
NIKHEF, National Institute for Subatomic Physics

December 15, 2015

Abstract

In this report, the possibilities of identifying a specific τ neutrino signature using KM3NeT, a neutrino telescope with an instrumented volume of multiple cubic kilometers, are investigated. When uniquely identified, these neutrinos can offer a unique view on the universe with little to no background.
We study the 'Double Bang' signature of the τ neutrino interaction and reconstruct these events with a reconstruction algorithm designed for single showers. Using this algorithm, the two particle showers in this event are reconstructed as a single shower. By looking at the differences in reconstruction performance between these events and single shower events, a first indication of the relevant parameters for the identification of τ neutrinos is given.

Contents

Chapter 1

Introduction

Neutrinos are neutral leptons with close to zero mass. They come, like all leptons, in three flavours, e, μ and τ . Neutrinos only interact via the weak interactions. Because of this and their small mass they have a small probability to interact with surrounding matter. This makes the neutrinos hard to detect. Neutrinos are created in many highly energetic processes in a range of active areas in the universe. By detecting neutrinos and assessing their properties (flavour, energy and origin) we can obtain information on the central regions of these areas, from where almost no light reaches us. Neutrinos can also give us information on very distant parts of the universe, since they can travel undisturbed across great distances.

Neutrinos are most commonly detected through the charged secondary particles that are created in their interactions. By studying the energy and direction of these secondary particles, the energy and type of the neutrino can be deduced.

Currently, a new project is under way to study high energy neutrinos using the detection of these secondary particles: KM3NeT. This project consists of the construction of a neutrino detector in the Mediterranean Sea, comprising a volume of multiple cubic kilometers. This volume will be filled with photo detectors which will detect radiation coming from the collision products from neutrino interactions. Using this detector, the KM3NeT project will be able to look at astronomical objects using neutrinos instead of photons as messengers. The construction of the KM3NeT detector has just started and the first experiments are in place for testing.

In this report, it is shown how the completed KM3NeT detector will be able to detect one specific flavour of neutrinos: the τ neutrinos. These neutrinos are especially interesting since atmospheric background for these particles is very low compared to the other flavours of neutrinos. This

Version of December 15, 2015– Created December 15, 2015 - 13:13

atmospheric background mainly consists of neutrinos created in processes that occur in the atmosphere. The energies in the typical atmospheric reactions is insufficient to produce τ neutrinos.

This report demonstrates the performance of `AAShowerFit` [1], an existing shower reconstruction algorithm, in reconstructing τ neutrino events. By applying the reconstruction algorithm to neutrino events, we can obtain information on the energy and direction of the neutrino. In this research, `AAShowerFit` was used on simulated data to assess the performance.

`AAShowerFit` was designed to reconstruct Charged Current electron neutrino showers. In these events, an electron neutrino interacts with a proton or neutron and produces a multitude of particles, moving in different directions; we call this a shower. For Charged Current electron neutrino events, all energy in the interaction is deposited in this shower. τ neutrinos show a different signature. When they interact with a proton, a shower and a τ lepton are created. This τ lepton can travel several meters, depending on its energy, before it decays into a muon, or creates a second shower (Double Bang). These decay paths produce significantly different signals from the electron neutrino showers.

Reconstructing Double Bang events, as are observed in τ Charged Current interactions, comes with new difficulties. Because the reconstruction algorithm assumes a single shower, the reconstructed position, direction and energy of the shower behave differently from single shower reconstructions when the two showers are separated by a distance bigger or equal to the extension of the shower. This property of the reconstruction, and the difference in quality parameters resulting from the difference in behaviour, could be used to distinguish double shower τ neutrino events from single shower events. In this report, it is shown that especially the position reconstruction loses accuracy due to the single shower approximation. Because the reconstruction algorithm uses the hits of two showers to reconstruct a single shower position, the result of this reconstruction will be distorted and the reconstructed position will no longer match the position where the neutrino interacts with the water. It is shown that the position `AAShowerFit` reconstructs is often closer to the τ decay vertex than it is to the neutrino vertex. The reasons for this property are explored.

Finally, first steps are reported towards the identification of τ neutrino events where two showers are observed. For this, the likelihood, angular error and reconstructed energy, output values of `AAShowerFit` , are compared between τ neutrino events with two showers and events where an electron decays via a Charged Current interaction to one shower.

Lepton	mass [MeV/c^2]	Mean lifetime	Neutrino mass
e^-	0.51	$> 4.6 \times 10^{26}$ yr	$< 2eV/c^2$
μ^-	105.66	2.20×10^{-6} s	$< 0.19MeV/c^2$
τ^-	1776.82	290.6×10^{-15} s	$< 18.2MeV/c^2$

Table 1.1: Some properties of the three flavours of leptons.[3]

1.1 Motivation

This report will focus on the reconstruction and identification of τ neutrino events. We will therefore first explain further why this flavour of neutrinos is interesting and what distinguishes it from the others.

τ neutrinos are different from the other flavours because of the high mass of their charged counterparts: the τ lepton. The properties of the three different types of leptons are summarized in Table 1.1. Because the τ-lepton is so much heavier than the leptons of other flavours, extremely high energy reactions are needed to create them. Most atmospheric interactions occur when cosmic rays hit the protons in the atmosphere. This mainly creates pions. These pions later decay to produce muons or electrons, but have insufficient mass to create τ leptons. Because particles of higher mass are needed (e.g. charm quarks) for the creation of τ leptons and neutrinos, only extremely highly energetic cosmic rays can produce these. This leads to a very high significance of τ neutrino signatures due to the absence of atmospheric background in the τ channel; when we detect such an event, we can be sure that it is a valuable signal and not background noise [2].

A possible problem with τ neutrinos is exactly this fact that extremely high energies are needed to create them. This could cause very few τ neutrinos to be produced in the cosmic accelerators which should be studied, simply because the reactions in these areas do not reach the energies needed. This problem is solved by the neutrino mass. Lately, it has been shown that neutrinos are not massless, but carry a very small mass. This has been shown by observing neutrino oscillations [4]. The neutrino are so small that they have not been measured accurately, but neutrino oscillations have given us the upper bounds shown in Table 1.1. The flavour eigenstates of the neutrinos do not coincide with their mass eigenstates. This means that when a neutrino is created in a certain flavour eigenstate it is in a mixture of mass eigenstates. In its lifetime, this mixture of mass eigenstates will oscillate, thereby also changing the probability to detect a certain flavour eigenstate. In this way, the flavour eigenstates oscillate between the three possible flavours.

Neutrinos from galactic sources are, according to the current theories, created in a 1:2:0 ratio for e-, μ- and τ neutrinos respectively. This ratio has been calculated using pion decay [8], where a charged pion decays into a (anti-)muon and a μ (anti-)neutrino. The muon created here then decays into an electron, a μ neutrino and an e anti-neutrino. Due to neutrino oscillation, this ratio will shift during the travel path of the neutrinos to a 1:1:1 ratio, where each neutrino flavour is equally probable, by the time the neutrinos reach earth. The intensity of these events can be calculated trough the decay of neutral pions into two photons, which are observed as gamma rays. For atmospheric neutrinos, the distance they travel is too low for the slow oscillations to be expressed. This is why almost no τ neutrinos are expected from atmospheric events due to oscillations.

One third of all galactic neutrinos reaching Earth are thus τ neutrinos, while almost no τ neutrinos are created in cosmic-ray interactions in the atmosphere. This makes the τ neutrinos an ideal candidate to probe active areas in the universe, combining the advantages of neutrinos; almost no disturbance by the galactic medium, with a very low background.

Version of December 15, 2015– Created December 15, 2015 - 13:13

Chapter 2

Neutrino Astronomy

Classically, astronomy has been performed purely by observing electromagnetic radiation, and although this approach has yielded great results, there are still parts of the galaxy that can not be explored in this manner. Big clouds of interstellar dustcan block the passage of photons and the high mass at their creation point can prevent them from escaping the object they originated from. Neutrinos can provide an alternative to photons as messengers of information from these dense, active areas.

Neutrinos have neutral charge and will therefore travel in straight lines from their origin to Earth. They only interact via the weak interaction and have a small interaction cross-section, allowing them to travel great distances before interacting. The interaction cross-section of a particle is a measure for its chance to undergo an interaction with a passing particle. Therefore, they are able to escape dense galactic regions from where we can see no electromagnetic radiation. Neutrinos are created in all active galactic areas such as supernova remnants, micro-quasars and Active Galactic Nuclei. In addition, we might see a flux of neutrinos coming from yet undiscovered sources which can not be probed using photons and are therefore unknown to us at the moment.

Although there is an abundance of highly energetic neutrinos reaching the Earth, their detection is challenging. Because they solely interact weakly, only a small fraction of all neutrinos reaching earth will interact to produce detectable particles. By having a huge instrumented volume (multiple cubic kilometres), KM3NeT, the detector discussed in this report, will have enough events to positively identify galactic point sources within a few years [8].

The following section will explain what kinds of detectable particles are created when a neutrino interacts with matter on earth. As a reference for

this and following chapters, the textbook on elementary particles by David Griffiths [5] was used.

2.1 The Weak Interaction

Neutrinos are neutral leptons, and will therefore not emit any radiation when they travel trough matter. To detect them, we use the products of their interaction with the protons and neutrons in the detection volume. In this section, the different types of interactions the three flavours of neutrinos can undergo will be explained.

Neutrinos only interact via the weak interaction, this interaction is mediated by the Z- and $W^{\pm}$ bosons. The first of these bosons carries no electric charge, whereas the W-bosons have a charge of $\pm e$, with e the elementary (electron) charge. These bosons are heavy with respective weights around 91 GeV and 80 GeV. This is one of the reasons that weak processes have, in general, a small cross-section.

The neutrino interactions will be explained by Feynmann diagrams. In Feynmann diagrams, each line represents a particle, and crossings of lines represent interactions. These interaction crossings are called vertices. For the weak interaction, there are three possible vertices, these are drawn in Figure 2.1. Interactions concerning the exchange of a W-boson are called Charged Current interactions, and those exchanging a Z-boson are called Neutral Current interactions.

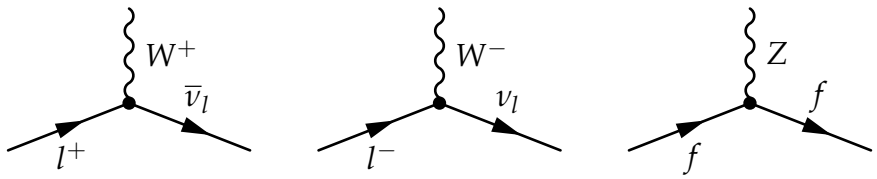

Figure 2.1: The elementary vertices for the weak interactions. Here, l is a lepton of any flavour and ν_l is the corresponding neutrino, f is any lepton or quark. $W^{\pm}$ and Z are the weak-interaction bosons.

As we can see from these vertices, the Neutral Current interactions do not change the particles in the interaction (Flavour Changing Neutral Current interactions have been predicted theoretically, but have not been observed so far). When a neutrino interacts via a Neutral Current process, it can interact with any particle, transferring some of its momentum to this particle. This interaction only changes the momentum of the particles and

not the particles themselves. A diagram of a Neutral Current interaction of a neutrino is shown in Figure 2.2a.

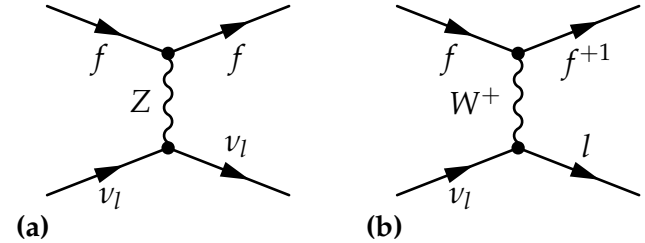

Figure 2.2: The neutral- (a) and Charged Current (b) interactions of a neutrino, Here, f is any quark or lepton and where relevant its charge is given as a superscript, ν_l is a neutrino of any flavour and l is the corresponding lepton.

The Charged Current interactions however, do change the particles included in the interaction. The W-boson moves one unit of charge from one particle to another. This turns a lepton into a neutrino, an anti-lepton into an anti-neutrino or an up quark into a down quark. An example diagram if this is shown in Figure 2.2b. In a Charged Current interaction, the neutrino is converted into a lepton of the same flavour as the original neutrino, the neutrino itself will not come out of the interaction.

2.2 Neutrino Interactions in Water

Now the basics on the weak interactions of neutrinos have been covered we look at the specific situation for the KM3NeT detector. Since the detector is in water there is an abundance of protons and neutrons in the vicinity of the detector. In the case of an interaction, we can therefore expect the neutrino to interact with either a neutron or a proton. In the case of Neutral Current interactions, the neutrino interacts and flies off again. This results in the hadron gaining momentum. When the energy of the neutrino is high enough, the momentum transferred to the hadron will cause it to decay in a hadronic shower of many charged particles. These charged particles move with velocities higher than the speed of light in water and thus produce Cherenkov radiation that can be detected, as will be described in section 3.1. This process is identical for all flavours of neutrinos and can therefore not be used to uniquely distinguish the τ neutrinos. However, it does give us information on the interaction vertex position and direction of the neutrino. The information on the energy of the neutrino we can determine from these events is limited, because the neutrino moving away carries an unknown amount of energy still with it.

The Charged Current interaction behaves differently. In this case the hadron affected will also produce a hadronic shower, but there is also a charged lepton produced in this interaction. These leptons behave differently depending on their flavour, therefore these interactions can be used to distinguish the neutrino flavours. An electron that is produced in this interaction will have such a high momentum that it produces bremsstrahlung. This radiation consists of high energy photons capable of pair production. The electron and positron created in this way will also exhibit bremsstrahlung and therefore we see an electromagnetic shower in which a great number of electrons and positrons are created in a short time, all of them producing detectable photons. The signal from an electron neutrino is therefore hard to distinguish from the Neutral Current interaction since the created electron will immediately produce this electromagnetic shower, such that only one (combined) shower is visible.

The interaction with a muon neutrino produces a muon. This muon loses less energy than the electron due to bremsstrahlung because of its higher weight. It can therefore travel throughout the volume of the detector, emitting Cherenkov radiation along its path. This radiation is detected and the path can be reconstructed from the signal. Eventually, the muon will decay, producing a (hadronic or electromagnetic) shower. The travel length of a muon of a typical energy of 1 TeV is a few kilometers.

Finally, the interaction with a τ neutrino will produce a τ lepton. This lepton is very heavy compared to the other two leptons and therefore its lifetime is a lot shorter. When it decays it can produce a shower, just as the muon, or it decays into a muon. The first case would be visible as two showers with a separation dependent on the τ travel length which is around 50 m for τ neutrino's with an energy of 1 PeV. The second shower, where the τ lepton decays, will produce less light due to neutrinos being produced. This decay path has been called the "Double Bang"[2]. The second case would be visible as a shower, from which a τ track originates. Later on, the τ lepton decays into a muon, which is brighter than the τ track. The muon emits more Cherenkov radiation because of its higher momentum. This decay path has been called the "Sugar Daddy" signature[2]. An overview of the different charged-current interactions of neutrinos is shown in Figure 2.3.

For Charged Current events, the interaction products of neutrinos of different flavours differ. These different products could be used to distinguish the three flavor neutrinos in KM3NeT.

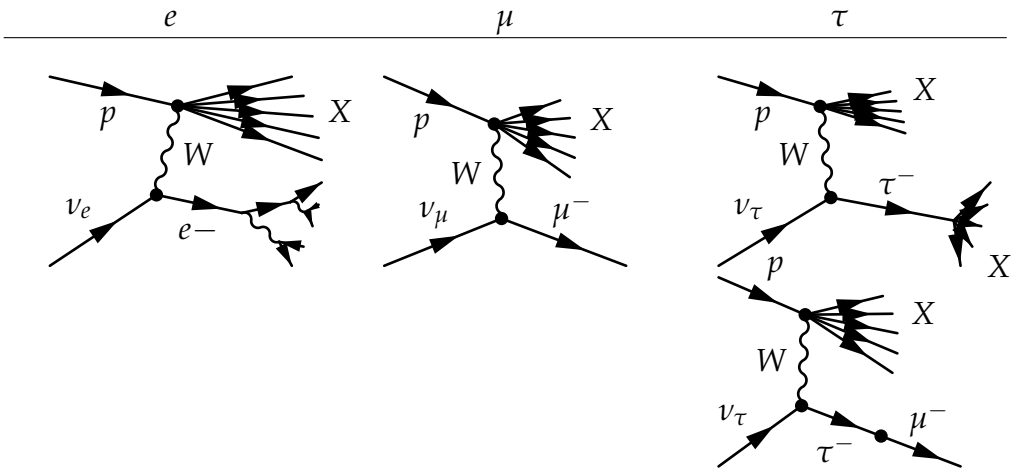

Figure 2.3: The Charged Current interactions of the three flavours of neutrinos with protons. Hadronic showers are denoted with X, and electronic showers are partly shown. Since the τ neutrino has two decay paths, both are shown. For the τ decay into a shower, a hadronic shower is shown, but it could also be an electromagnetic shower.

Chapter 3

KM3NeT

This section will provide basic information on the KM3NeT detector. KM3-NeT is a Cherenkov detector which will be used to detect neutrinos. All information in this section has been adapted from the conceptual and technical design reports of the KM3NeT collaboration [6, 7] and the later status update [8]. For a complete description of the KM3NeT detector, refer to those publications.

KM3NeT is a deep-sea observatory that is being built in the Mediterranean sea. Its main goal is to detect galactic neutrinos by looking for the Cherenkov radiation produced by the charged products of interacting neutrinos. For this purpose, the total instrumented volume of KM3NeT will be multiple cubic kilometres, composed of six building blocks with approximately one cubic kilometre of instrumented volume each. A more extensive description of the KM3NeT design is presented in section 3.2.

The enormous volume of KM3NeT will provide the collaboration with a high event rate and the set-up with many photodetectors will provide accurate angular and spatial resolution. The three locations of KM3NeT have been chosen according to the locations of the previous neutrino detector experiments: ANTARES (20 km south of Toulon in France), NEMO (100 km from Capo Passero in Sicily) and NESTOR (30 km southwest of Pylos in Greece). During these experiments extensive research has been done on the characteristics of these locations and that information can now be used for the construction of KM3NeT. Another advantage of these locations is that the KM3NeT will complement the view of IceCube, which is situated in Antarctica, on the sky, offering a window on, among others, the galactic centre.

Another project that is an integral part of KM3NeT is ORCA[9]. In this project, the KM3NeT detector will be used to accurately measure low

energy neutrinos, with energies between 3 GeV and 20 GeV. By accurately measuring the energy and zenith angle of these neutrinos, information can be gained on the ordering of the neutrino masses.

The enormous volume of the detector will not only be used for neutrino astronomy, but will also facilitate several projects in the fields of environmental sciences, geology, marine biology and oceanography. The cabled infrastructure, with a constant supply of power and a way to send data to shore, presents a unique opportunity to study the Mediterranean sea for longer periods of time. Most current investigations have only had the possibility to use autonomous observation stations with lifetimes of maximally one year.

The KM3NeT collaboration consists of teams from three previous generation neutrino experiments: ANTARES, NEMO and NESTOR, of which only ANTARES was fully realized. Know-how from these three teams is combined in the construction of KM3NeT to make the system not only accurate in detecting neutrinos, but also robust against the rough deep-sea environment.

3.1 Cherenkov Detectors

High-energy charged particles moving through water, such as the interaction products described in the previous chapter, will surpass the speed of light in water, as this speed is 'only' $0.75c$. When this is the case, an electromagnetic version of the sonic boom occurs: Cherenkov radiation [10]. This radiation has a distinct spectrum which is the most intense in the short-wavelength part of the spectrum. This spectrum is given by the Frank-Tamm formula, which describes the number of photons emitted from a charged particle (N) per path length (x):

$$\frac{d^2N}{dxd\lambda} = \frac{2\pi\alpha}{\lambda^2}\left(1 - \frac{1}{n^2\beta^2}\right) \tag{3.1}$$

where λ is the Cherenkov photon's wavelength, α is the fine-structure constant and β is the speed of the particle divided by the speed of light in vacuum ($\beta = \frac{v_p}{c}$).

In nuclear reactors, Cherenkov radiation in water can be seen as a brilliant blue light, but for most particles the visible part of the spectrum is too faint to be seen by eye. The wavelength of the light used by most Cherenkov detectors lies around 450 nm. This wavelength is dictated by the absorption spectrum of water, causing the resulting Cherenkov spectrum after absorption to be at a maximum around this wavelength. The

Cherenkov light is emitted at a distinct angle around the travel path, similar to the cone of sound waves sonic booms produce. This angle is given by

$$\theta_C = \frac{1}{n\beta} \tag{3.2}$$

where n is the refractive index of the medium ($n \approx 1.35$ for sea water). For highly energetic particles, $\beta \approx 1$, the Cherenkov angle will approach $\theta_C = 42^\circ$ and becomes independent of the particles energy.

Water Cherenkov detectors use this light to detect the high-energy charged particles. An array of sensitive photo detectors is placed in or around a volume of water and when a charged particle moves through the water these detectors will detect the Cherenkov light. By using the time, position and direction information of the hits on the photo detectors, combined with the known Cherenkov angle at which the light is emitted, charged particles moving trough water can be tracked within the detector. In this way both tracks (particles moving through the detector for a long time) and showers (sudden bursts where many short-lived particles are created) can be studied.

Although in the preceding text only water-based Cherenkov detectors are discussed, any transparent medium with a sufficiently high optical index can be used in the volume of a Cherenkov detector. For instance, a Cherenkov detector has been constructed in the ice of Antarctica: IceCube [2].

3.2 Technical Design

For the KM3NeT telescope, optical modules have been designed to contain the individual photo detectors. These Digital Optical Modules (DOMs) consist of 31 photo multipliers with a diameter of 3 inch contained in a 17 inch sphere. The photo multipliers are positioned in the sphere equally distributed in both angles that span the sphere. An image of a DOM is shown in Figure 3.1b.

Photo multipliers detect incoming photons by multiplying the electrons a photon excites in a metal receptor material through a process called secondary emission. After multiplication, these electrons are then accelerated to the next receptor, where the same process occurs. This is done multiple times, each time enhancing the signal. An image of one PMT is shown in Figure 3.1a.

The configuration with multiple PMTs on a DOM was preferred over a configuration with large single-PMT DOMs, as have been used in previous

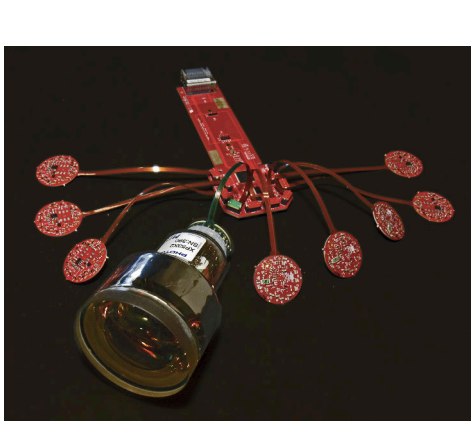

(a)

(b)

Figure 3.1: Images of a single Photo Multiplier Tube (PMT) attached to a control board (3.1a) and a Digital Optical Module (DOM) (3.1b), in which 31 PMTs are assembled. *Source: Propriety KM3NeT Collaboration*

experiments, because of the possibility to correlate the hits on a DOM. Correlation of hits can help in filtering out random noise caused by the PMT electronics, ^{40}K decay and bioluminescence. The background signals for Cherenkov Detectors are described in more detail in Section 3.4.

18 DOMs are attached on a string, with a spacing between the DOMs of 36 m. The string is attached to an anchor which will be sunk to the bottom of the ocean. The string is then kept taut by a system of buoys attached above the highest DOM, as well as the buoyancy of the DOMs themselves. This makes for a vertical string of detection units, looking at all directions.

For deployment, these strings are rolled up in a Launcher for Optical Modules (LOM). This LOM has been designed to sink to the bottom of the sea and there unroll the string in a controlled manner. After the deployment of the string, the LOM resurfaces and can be reused.

Multiple strings are placed together, with a horizontal separation of 90 m, forming a three dimensional grid of DOMs. The full KM3NeT detector will consist of multiple building blocks, where each building block consists of 115 strings. An artists impression of such a building block is shown in Figure 3.2.

Constructing KM3NeT as a structure of strings enables the collaboration to place individual strings into place as soon as possible. Each string can be controlled individually, and measurements will begin as soon as one of the strings is in place. This provides the collaboration with valuable data

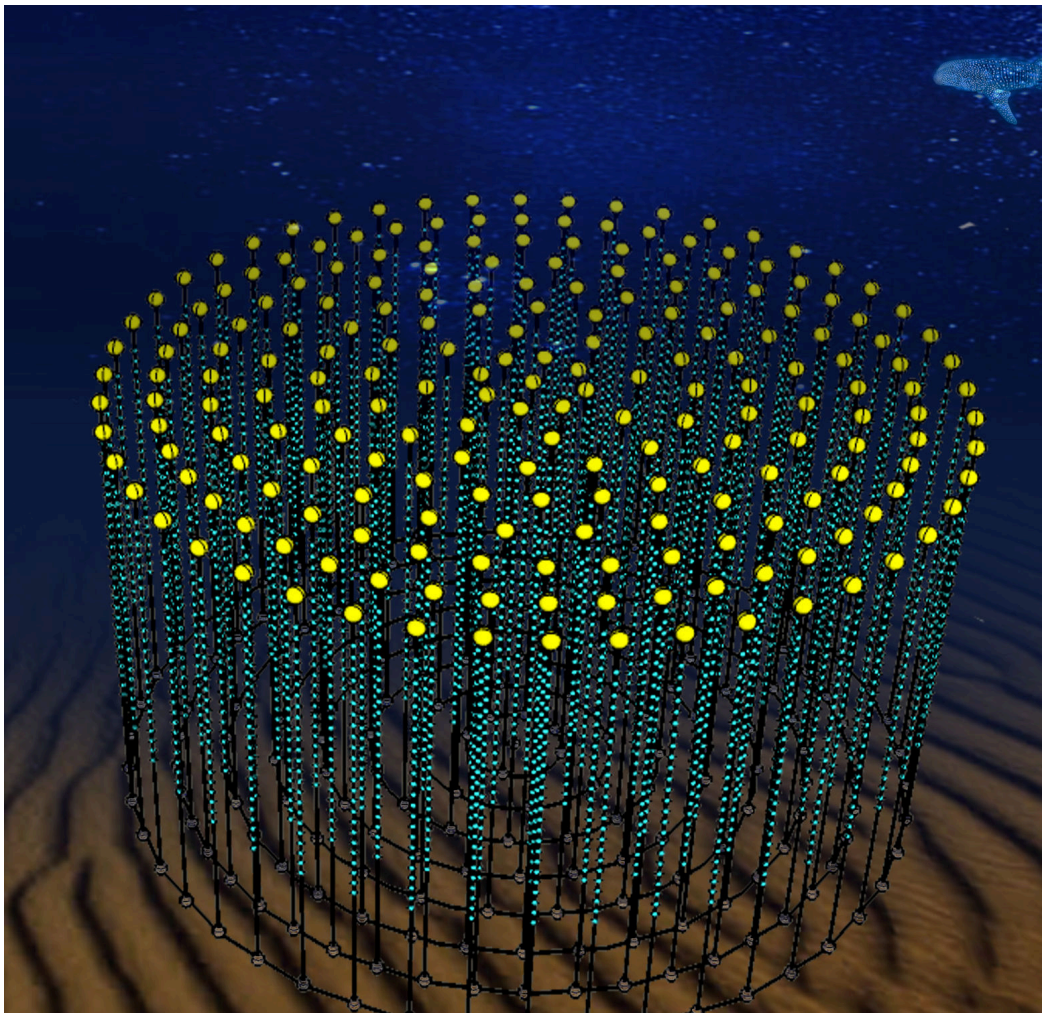

Figure 3.2: An artists impression of one building block of KM3NeT. DOMs are shown in blue, and the buoys are shown as yellow spheres. *Picture courtesy: Marko Kraan (NIKHEF)*

early on in the building process. Currently, tests are already running with as little as three DOMs on a small string [8].

The choice to construct the KM3NeT telescope out of building blocks was made to be able to position the detector in multiple sites. It has been shown that, as long as each building block has a size bigger than $0.5\,\mathrm{km}^3$, the distribution of the blocks no longer influences the performance. Eventually, the telescope will consist of six building blocks, situated in three different locations, amounting to a total instrumented volume around three cubic kilometres.

Currently, the first 31 strings are under construction and will be deployed at the French and Italian sites in 2015-2016. [11].

3.3 Neutrino signals

In KM3NeT the charged particles moving through the detector are detected by the Cherenkov light they emit. For Neutral Current events, as stated in section 2.1 we can not see any differences between the neutrino flavours because they all create hadronic showers. For Charged Current events however, this is possible.

Muons have the most characteristic signature. Muons have a long lifetime (2.2 µs, without taking relativity into account), at the relevant energies this translates to travel lengths of several kilometers in the water. The Cherenkov light they emit along their path can be reconstructed using the timing information of the hits. Good results on this reconstruction have already been obtained even in smaller detectors like Antares, the predecessor of KM3NeT with a volume of around 0.05 km^3. An example of what a muon neutrino event could look like in the KM3NeT detector is shown in Figure 3.3. All figures in this section are based on the Monte Carlo simulations described in section 4.1.

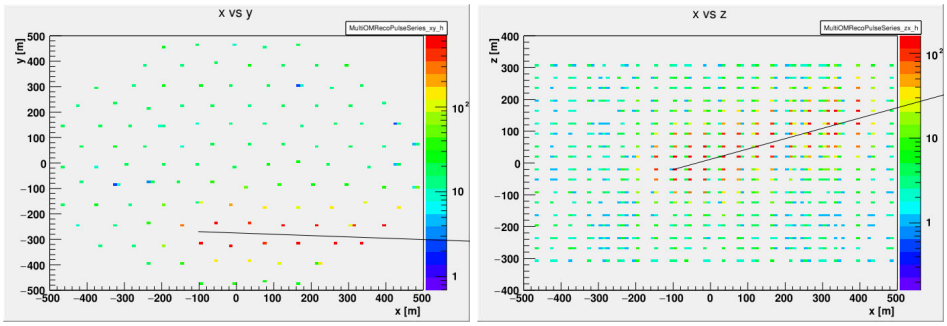

Figure 3.3: Event displays of a Charged Current muon neutrino event in one building block of the KM3NeT detector, of which a top view (x vs y) and a side view (x vs z) are shown. For the show event, the decay of the muon neutrino happened inside the detector volume. An arrow is drawn to indicate the flight path of the muon created in the interaction. The coloured dots show the positions of the PMTs, their color indicates the number of hits on that PMT.

Although the highly energetic muon track is easily recognized, it is not always a clear indication that a muon neutrino caused it. τ leptons created in the decay of a τ neutrino can, as we have seen in the previous section, decay into a muon. This muon will also leave a track in the detector.

An example of such an event is shown in Figure 3.4. The only way to distinguish these two types of events is when the initial shower is contained within the detector and the τ lepton travels long enough so that we can see the creation of the muon separately from the shower.

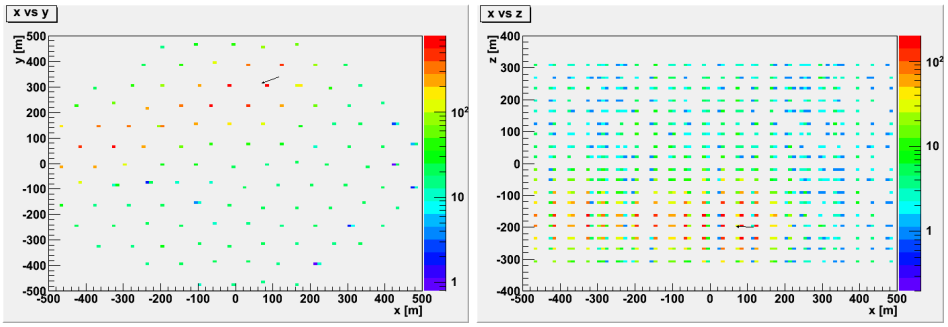

Figure 3.4: Event displays of a Charged Current τ neutrino event where the τ lepton decays into a muon in one building block of the KM3NeT detector, of which a top view (x vs y) and a side view (x vs z) are shown. An arrow is drawn to indicate the flight path of the τ lepton created in the interaction. The coloured dots show the positions of the PMTs, their color indicates the number of hits on that PMT.

Electron neutrinos entering the detector will cause an electromagnetic shower. An example of this is shown in Figure 3.5. Such a shower without a track coming out of it is different from the previous two events described above. It is, however, not unique. A τ neutrino entering the detector will produce a shower and a τ lepton, which soon thereafter produces a shower. If the path length of the τ lepton is short, the event is hardly distinguishable by eye from an electron shower, as can be seen in Figure 3.6.

When the energy of the incoming τ neutrino is higher however, the τ lepton can travel further and the two showers are distinguishable by eye, see Figure 3.7. This is a promising way to uniquely detect high energy τ neutrinos and it is what the remainder of this report will focus on.

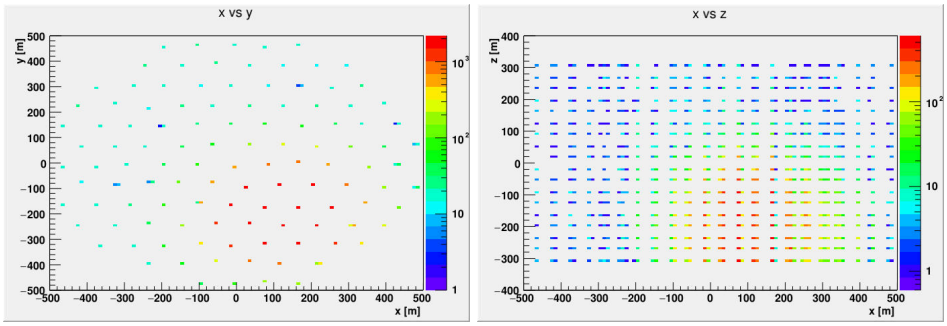

Figure 3.5: Event displays of a Charged Current electron neutrino event in one building block of the KM3NeT detector, of which a top view (x vs y) and a side view (x vs z) are shown. The coloured dots show the positions of the PMTs, their color indicates the number of hits on that PMT.

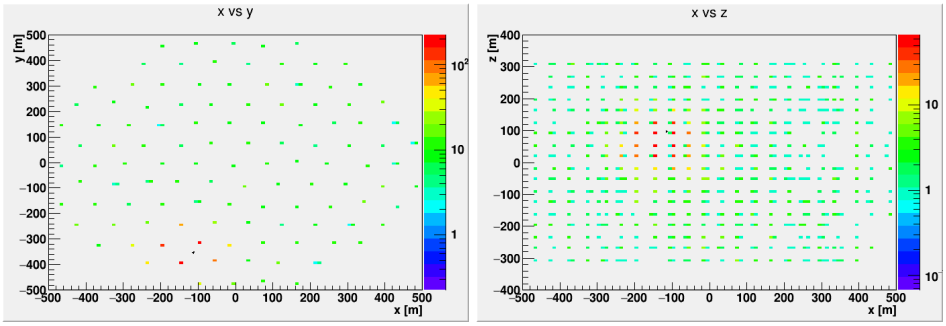

Figure 3.6: Event displays of a Charged Current τ neutrino event where the τ lepton decays into a shower in one building block of the KM3NeT detector, of which a top view (x vs y) and a side view (x vs z) are shown. An arrow is drawn to indicate the flight path of the τ lepton created in the interaction. In this event, the travel length is 0.431 m The coloured dots show the positions of the PMTs, their color indicates the number of hits on that PMT.

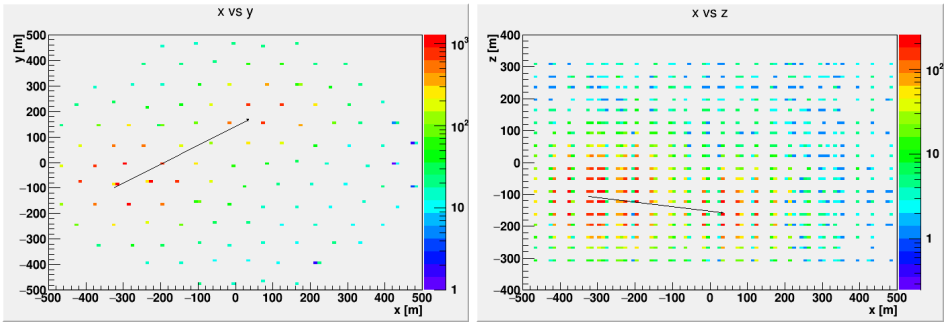

Figure 3.7: Event displays of a Charged Current τ neutrino event where the τ lepton decays into a shower in one building block of the KM3NeT detector, of which a top view (x vs y) and a side view (x vs z) are shown. An arrow is drawn to indicate the flight path of the τ lepton created in the interaction. In this event, the travel length is 450.555 m The coloured dots show the positions of the PMTs, their color indicates the number of hits on that PMT.

3.4 Background

As with any detector, Cherenkov detectors also obtain signals from background. In this section the different background signals will be explained and the design choices to minimize the effect of this background are discussed. This discussion is based on background section of the Performance Studies for KM3NeT [12].

First of all, there is background noise from the direct environment, in the case of KM3NeT the sea. KM3NeT is located deep enough under the sea level to eliminate any light coming from the surface, but there are also sources of light in the sea itself. On of these is the decay of ^{40}K isotopes in the sea salt. These unstable isotopes will undergo β-decay with a probability of around 90%, producing an electron with an energy of around 1 MeV, which will create Cherenkov radiation. In almost all other cases, the ^{40}K atom will decay to ^{40}Ar, which will in its turn emit a high energy photon which can create electrons via Compton-scattering. This is observed as a random background noise with a constant count rate around 5 kHz per PMT. This effect is observed throughout the detector.

Another background is caused by bioluminescence. Both bioluminescent bacteria and larger organisms cause this background signal. The bioluminescent background has been measured by ANTARES to have a baseline noise rate of about 60 to 120 kHz with occasional bursts increasing the noise rate to over a MHz. These bursts have durations of up to a few seconds.

To correct for the random background signal from ^{40}K decay and bioluminescence, triggers are applied which select time coincident PMT signals. This way, only signals that are recorded by at least two PMTs within a time frame of 25 ns are admitted. After this, the coincident hits are correlated between DOMs to further suppress this background signal.

Atmospheric neutrinos and muons form the second type of background signal. They are created when cosmic rays interact with the atmosphere. Atmospheric muons have a flux which is higher than that of atmospheric neutrinos by about 5 orders of magnitude at sea level. They are, however, highly attenuated by the sea water and the Earth. Therefore, there is little background of atmospheric muons coming from directions below the horizon. This makes it possible to distinguish a large part of the athmospheric events from signals induced by upward going particles.

The atmospheric neutrinos can not be distinguished from other neutrinos and are therefore an irreducible background. However, the interactions in the atmosphere that create neutrinos mainly create muon and electron neutrinos. The τ neutrino signal is therefore less contaminated by the

Version of December 15, 2015– Created December 15, 2015 - 13:13

atmospheric neutrino background. The atmospheric background from other neutrinos is decreased by selecting only neutrino events coming from within a specific cone when looking for point sources and later on subtracting the expected level of background hits.

Chapter 4

Simulation and Event Reconstruction

In this chapter, a brief description of the methods used to simulate and study neutrino events in KM3NeT is given. First, the Monte Carlo simulation chain used to generate neutrino events is explained, along with the cuts we make on the data. Secondly, `AAShowerFit` , the shower reconstruction algorithm used in this study, is explained and its performance on single shower events is shown. We conclude this chapter with some remarks about the used software and data formats.

4.1 Simulations

The data used for the following analysis is produced in the KM3NeT official Monte Carlo productions. Monte Carlo methods generate samples of probability distributions. In this case, the probability distribution is, among others, dependent on the position where the neutrino is created, the travel direction of the neutrino and its energy. Neutrino flavour and the decay mode could also be included in this distribution. The Monte Carlo method then picks one combination from this distribution at random and computes the path of the neutrino and the consequent signal in the virtual detector.

In the Monte Carlo productions, many of these samples are created. First a great number of neutrinos with energies ranging from 10^2 to 10^8 GeV are simulated some distance from the detector. The energies are distributed according to a predefined power spectrum. A histogram of such an energy spectrum is shown in Figure 4.1. These neutrinos are then propagated in random directions and those which enter "the can", a certain volume

around and including the simulated detector, are simulated to interact in this volume, the rest is discarded. The detector is simulated to resemble the latest layout of one building block of KM3NeT, as described above. These decays are then propagated through the detector. There, the Cherenkov light from the charged particles is simulated. Finally, the detector elements are taken into account and the electronics of the PMTs are simulated to obtain realistic signals.

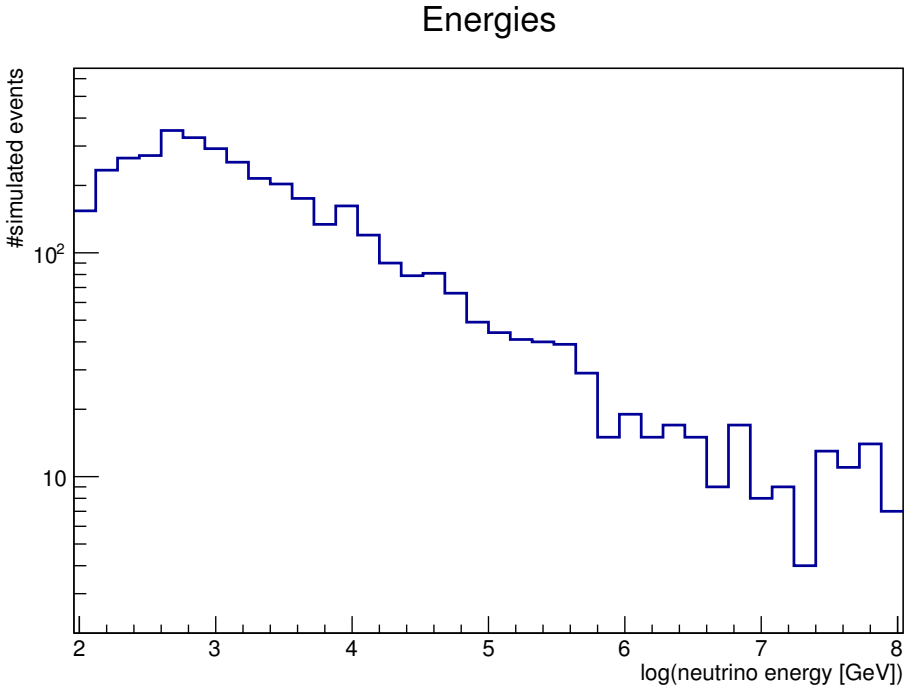

Figure 4.1: A histogram of the energies of the simulated neutrinos in one Monte Carlo simulation file containing 9478 events. The simulated interaction for this file was τ neutrino Charged Current, where the resulting τ lepton only decayed as a shower.

The simulations are generated by a production chain. The first part of the simulation is done by `GENHEN`[13] (GENerator of High Energy Neutrinos), which generates the neutrinos. Next, the light is propagated trough the detector and the response of the detector is simulated by the `KM3`[14] package. This packages simulates the effect of the detector without having to keep track of all photons created in an event. In the last part of the production chain, `JTriggerEfficiency`[15] simulates the background light, such as potassium-40 decay, the PMT response and the triggering mechanisms of the detector.

The data samples are split up according to the type of neutrino (flavour and neutrino/antineutrino) and the type of interaction via which they decay. This makes it easy to compare the different neutrino flavours and decay paths. For τ Charged Current events, the data are split up again according to whether the τ decays into a muon or creates a shower. For the τ neutrino double shower events, 10^8 simulated events are recorded in one sample, for the other types, 10^5 events are recorded. The following investigations are done on 100 files for each of the interactions.

4.1.1 Containment Requirement

To ensure reliable data for which a sensible reconstruction is possible, a containment cut is applied on the events. Only events where the reconstructed neutrino interaction vertex fulfills the relations $\sqrt{x^2 + y^2} < 380\,\mathrm{m}$ and $|z| < 260\,\mathrm{m}$ (where x, y and z are the coordinates of the vertex with respect to the detector centre) are accepted. This cut ensures that the biggest part of the shower will be contained within the active detector volume. Figure 4.2 illustrates this containment requirement.

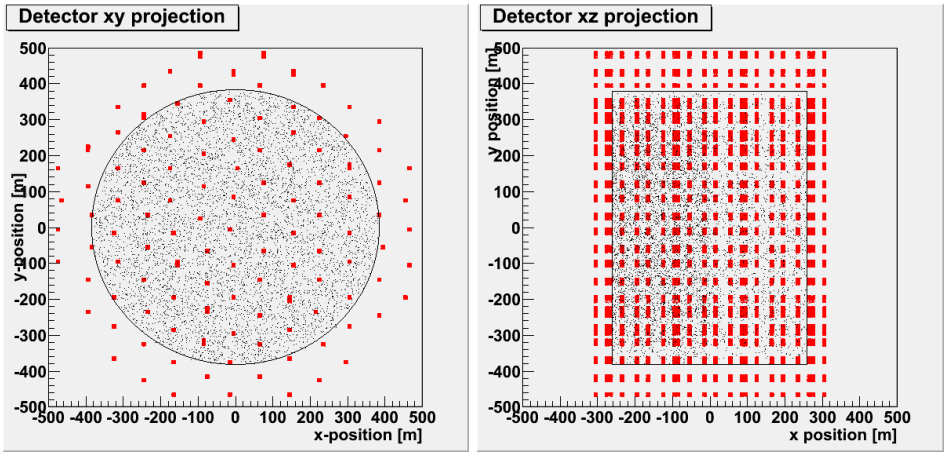

Figure 4.2: Layout of the KM3NeT DOMs (red) and an example of hits that make the containment criterion (black). The volume in which hits are accepted by the containment criterion is indicated by a black line. Distances are measured from the centre of the detector.

4.2 AAShowerFit

`AAShowerFit` is a shower reconstruction algorithm developed by Aart Heijboer[1]. It is designed to complement the existing accurate track fitters and has been shown to be able to accurately reconstruct the position of the interaction vertex and the direction and energy of the neutrino in Charged Current electron neutrino events.

To reconstruct the showers, it uses a multi-step procedure, which will be described below.

First, the hits on each PMT are merged. All hits occurring within 300 ns of each other are merged, retaining the time of the first hit to this PMT as the time of the merged hit.

Secondly, all hits on a DOM that occur within 20 ns are merged, these hits are called coincident. The number of merged hits is recorded as the multiplicity of this hit. The time of this hit is, again, set to the earliest PMT hit.

Thirdly, the position and time of the merged hit with the largest multiplicity is used as the start value for an M-estimator fit. The M-estimator fit is based on the assumption that even though the shower is extended, the hits will look like they are emitted from a single point source. Assuming this first coordinate, the deviation in arrival time for each of the hits is evaluated, based on the expected propagation time of the light in water. The usage of an M-estimator instead of the usual χ^2 fit has the advantage that it is less sensitive to outliers (hits that are uncorrelated to the vertex position).

The hits that are used as input for the M-estimator are those coincident hits that occur with an absolute time residual of less than 800 ns with respect to the first expected Cherenkov photon based on the first position and time estimate. Then, the following value is minimized for all selected hits:

$$M = \sum_{Hits} \sqrt{1 + r_i^2} \tag{4.1}$$

Where:

$$r_i = t_{hit} - |pos_{hit} - pos_{shower}|/v + t_{shower} \tag{4.2}$$

Here, t and pos are the time and position coordinates of either the hit, or the reconstructed shower, and v is the speed of light in water. This fit returns the position and time of the shower.

Version of December 15, 2015– Created December 15, 2015 - 13:13

Finally, subsequent fits are made to reconstruct the direction and energy of the incoming neutrino using all hits instead of the merged coincident hits used for the position reconstruction. For this, a probability density function (PDF) with four parameters is used:

- μ: the mean number of photoelectrons from a shower
- $r = |\mathbf{v}|$
- $z = \mathbf{d} \cdot \mathbf{v}/r$
- $a = \mathbf{k} \cdot \mathbf{v}/r$.

Where $\mathbf{v}$ is a vector from the shower centre to the centre of the optical module, $\mathbf{d}$ is the shower direction and $\mathbf{k}$ is the direction in which the PMT is looking. The energy dependence of μ is linear, following

$$\mu = \frac{E}{E_0}\mu^{E_0}(r, z, a). \tag{4.3}$$

Here, E_0 is any energy for which μ^{E_0} is known. In this case, μ^{E_0} was computed using Monte Carlo information for E_0 =1 PeV. The final fit is done by minimizing the likelihood given by

$$\log \mathcal{L} = \sum_{\text{empties}} \log[P_0] + \sum_{\text{hitPMTs}} \log[P_0 - 1]. \tag{4.4}$$

Where

$$P_0(r_i, z_i, a_i, E) = \exp[-\mu(r_i, z_i, a_i, E)] \tag{4.5}$$

This reconstruction is repeated twelve times, each time changing the starting direction for the minimizer to another point on an icosahedron. The value with the lowest likelihood is then chosen to be the final result.

After these reconstruction steps, a polynomial correction is applied to the reconstructed energy to correct for a negative bias in the reconstruction.

For Charged Current electron events, this procedure has shown to have good direction ($<1^\circ$) and energy resolution ($\pm 5\%$) for high energy (> 10 TeV) showers, see Figure 4.3. In this Figure, the black line shows the median of the data, and the spread of the data is indicated by the colored regions. We see that, especially for high energy events, the spread becomes small and the median is close to the known values for the incoming neutrino.

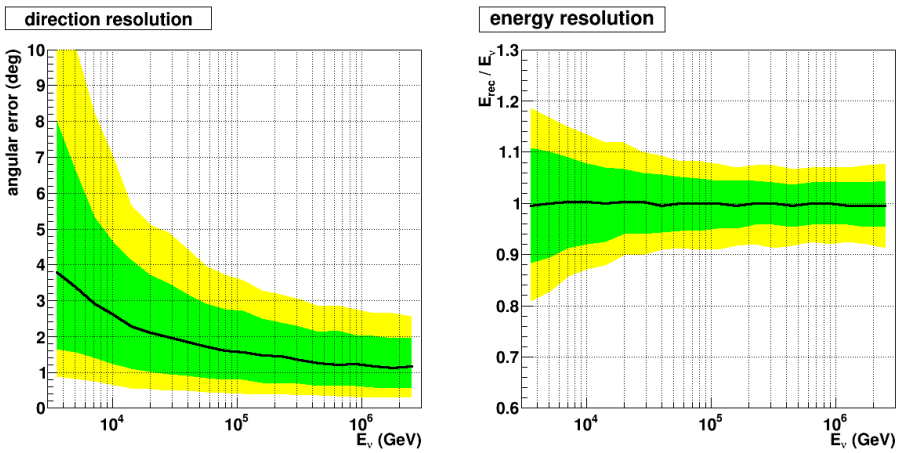

Figure 4.3: The energy and direction resolution reported for `AAShowerFit` by Aart Heijboer [1]. The median is indicated by the black line, and the green and yellow area's contain 68 and 90% of the distribution respectively. Shown are the angular error and the fraction of the reconstructed and the simulated neutrino energy, both as a function of simulated neutrino energy

With these great results, it is interesting to look at the performance of `AAShowerFit` on double-shower τ neutrino events. Since these events have two showers, the single shower assumption of `AAShowerFit` is likely to fail when the two vertices move more apart. For low energies, the vertices are close together and the reconstruction will work fine. For highly energetic τ leptons however, this distance becomes larger and it is expected that the performance of `AAShowerFit` will worsen. This would be visible in a greater spread of the quantiles for the position resolution at high energies.

4.3 Data Formats

The data from the Monte Carlo simulations is produced in JTriggerEfficiency's native data format. This is a `ROOT` TTree, containing all information on the detector hits as well as the Monte Carlo information on the particles that produced the hits. A hit is defined as a photon exciting enough electrons in a PMT to reach a set threshold. Each particle is stored as a track, with a unique particle ID, creation time, position, direction energy and type. For the τ particles the length of the track is also stored. For the hits, the hit time, the ID of the hit PMT and on which DOM it is located and the Time over Threshold (ToT) are stored. The ToT is the time, recorded by a PMT that the number of pulses created by the incoming light remains over

a set threshold. The ToT can be used to estimate the energy of a hit, where longer ToTs suggest higher energies. The exact relation between these two has not been established however. Therefore, the ToT is not used in the `AAShowerFit` reconstruction.

The results from `AAShowerFit` are written out as a `ROOT` TTree, where each event is stored separately along with the Monte Carlo information. The TTree used for this is different from the JTE data-format, but stores the same information. The Monte Carlo particles and the reconstructed shower are stored as Tracks, and the hits, when written to the file, are written as Hits. These classes are similar to the `JTE` classes.

Chapter 5

Results

In this research, a way to distinguish τ Charged Current showers from other types of showers (Neutral Current or electron Charged Current showers) based on a shower reconstruction has been explored. To do this, the performance of `AAShowerFit` at reconstructing these various shower events has been investigated, as well as some of the output values this algorithm produces. Results from both investigations will be presented in this chapter.

5.1 Performance

`AAShowerFit` has been shown to have great reconstruction performance for Charged Current electron showers [1], with an energy resolution of 5% and a direction reconstruction of a few degrees. Therefore, it is also expected to perform well on other single shower events, such as the Neutral Current showers from the three flavours of neutrinos. Its performance on double shower events, such as the τ Charged Current interactions, has not been investigated yet. In the following, the performance of the algorithm will be presented for both single- and double shower events.

To assess this performance, the reconstructed position, direction and energy are compared with the simulated position, direction and energy of the neutrino, know from the Monte Carlo information. In Table 5.1, the quantities that are used in this assessment are summarized. These quantities are plotted versus the true neutrino energy to distinguish the behaviour of the algorithm for different energy ranges.

As a control on the reconstruction algorithm and on the datasets, a reconstruction on datasets of single shower events was first performed. The single shower events investigated are the electron, muon and τ Neutral

Variable	Function	Units
Deviation in position	$\lvert\overrightarrow{pos}_{rec} - \overrightarrow{pos}_{mc}\rvert$	m
Deviation in energy	$\frac{E_{rec}-E_{mc}}{E_{mc}}$	
Deviation in direction	Angle $\left(\overrightarrow{dir}_{rec}, \overrightarrow{dir}_{mc}\right)$	degrees

Table 5.1: The variables used in the assessment of the performance of `AAShowerFit`

Current showers and the electron Charged current showers. The performance of the algorithm in reconstructing the energy, direction and position of the shower is plotted in Figures 5.1, 5.2 and 5.3 respectively.

Comparing these plots, we see a very similar behaviour of the reconstruction of both the position and direction of the showers. The showers are accurately reconstructed at energies greater than 10^4 GeV. These results are in accordance to the reported performance of `AAShowerFit`.

When we take the energy reconstruction into account, there is a clear difference between the Neutral Current events and the Charged Current electron events. This can be explained by the nature of the interaction causing the shower. In Neutral Current interactions, the neutrino only transfers a part of its energy to the proton creating the shower. The rest of the energy is carried away by the outgoing neutrino. Therefore, we can not expect the reconstructed energy of these showers to be equal to the initial neutrino energy since there is no way to know how much energy is carried away by the neutrino. This also explains why the direction reconstruction performance is slightly worse for these events: there are less hits that can be used to reconstruct the direction for Neutral Current events than for Charged Current events, where all energy is converted into particles that cause hits in the detector.

For Charged Current electron showers, an electron is produced in the interaction so that all energy will be contained within the shower. Therefore, we can expect the reconstructed energy of the shower to be close to the neutrino energy in these cases, and this is confirmed by the performance shown in Figure 5.1d.

The reconstruction performance of the showers from the Neutral Current interactions for the three flavours of neutrinos is very similar. As was expected since the three interactions occur according to the same mechanism. The fact that the reconstruction does not distinguish these interactions is a confirmation of the validity of these Monte Carlo samples for the purpose of comparing the reconstructions.

With this confirmation of a valid comparison between the different Monte Carlo productions, the τ signature can be investigated. Electron

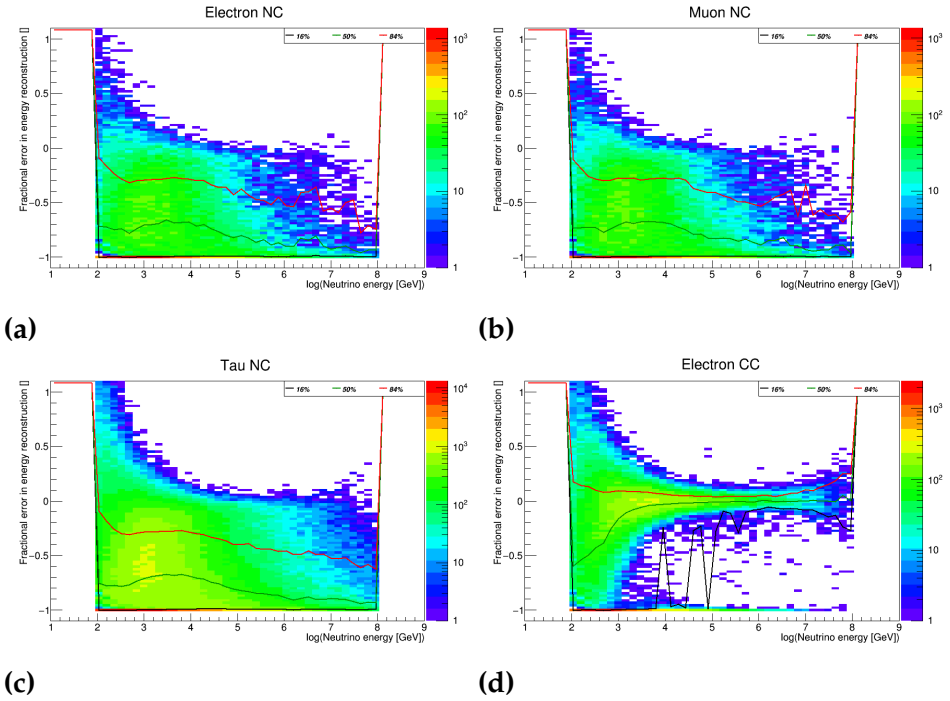

Figure 5.1: Performance of `AAShowerFit` in reconstructing the energy of electron (5.1a), muon (5.1b) and τ (5.1c) Neutral Current showers, and for electron Charged Current showers (5.1d). Shown is the fractional deviation with respect to the neutrino energy. The histogram entries are shown as a color map, and the 16%, 50% and 84% quantiles are drawn on top.

Charged Current events have been chosen as a baseline to investigate the performance of `AAShowerFit` at reconstructing the τ neutrino "double bang" signature. For τ neutrino Double Shower events, a large part of the energy will also be deposited in the two showers, which makes the Charged Current electron events a suitable baseline.

The performance of `AAShowerFit` for τ neutrino showers is shown in Figure 5.4, where they are compared to Charged Current electron neutrino showers and Neutral Current muon neutrino showers. There is little difference to be seen by eye in the reconstruction of the direction between the electron and τ showers, but the deviation of direction reconstruction on the muon neutrino showers is significantly higher. The position reconstruction for the electron and muon neutrinos show the same trend, but the τ neutrino direction reconstruction diverges from these curves around 1×10^6 GeV. This is the expected effect of the separation of the two showers. As the travel length of the τ lepton increases, the distance

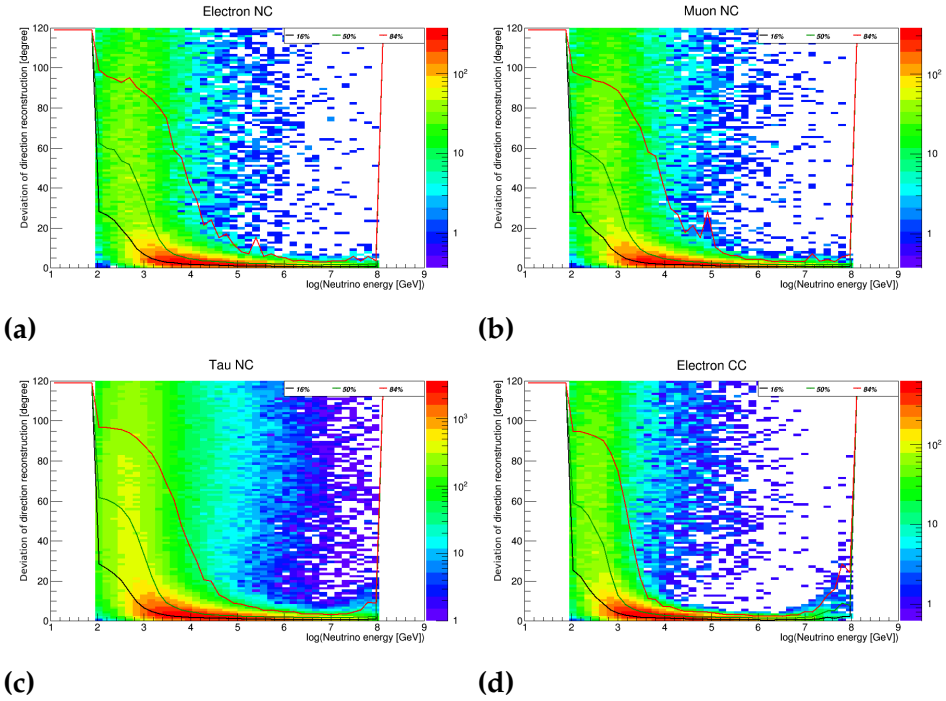

Figure 5.2: Performance of `AAShowerFit` in reconstructing the direction of electron (5.2a), muon (5.2b) and τ (5.2c) Neutral Current showers, and electron Charged Current showers (5.2d). Shown is the deviation between the reconstructed shower direction and the neutrino direction. The histogram entries are shown as a color map, and the 16%, 50% and 84% quantiles are drawn on top.

between the two shower vertices increases ($\text{len}_\tau(E_\tau) \approx \frac{E_\tau}{2 \times 10^4\,\text{GeV}} \cdot \text{m}$) and the assumption that the two showers can be reconstructed as one starts to fail. This effect does not affect the direction reconstruction because the second shower elongates the perceived combined shower, making the shower direction even more pronounced. The position reconstruction is affected however. As can be seen in Figure 3.7, the "double bang" events show two shower maxima, only one of them located around the neutrino vertex. `AAShowerFit` will fit the position of a shower maximum, but there is no control on which maximum it chooses. In the case of `AAShowerFit` choosing the second shower maximum, the reconstructed position will be away from the neutrino vertex by about the τ lepton travel length. This leads to the deviations we see in Figure 5.4b around neutrino energies of 1×10^6 GeV.

When we look at the energy reconstruction, we see that the electron Charged Current showers are reconstructed well and that the reconstruction performs worst for the muon Neutral Current showers. This is caused

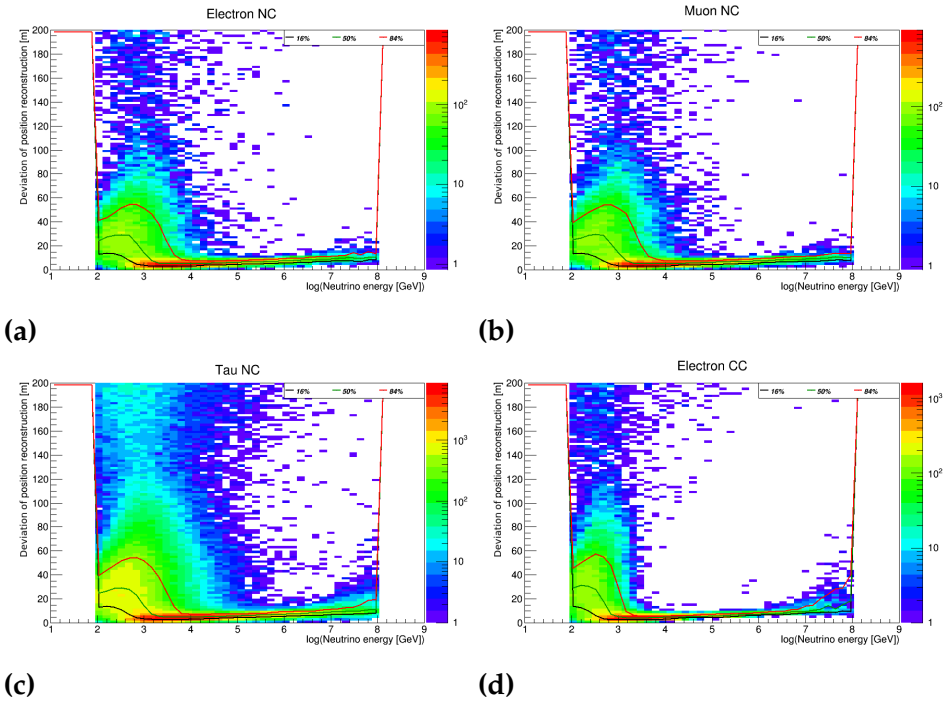

Figure 5.3: Performance of `AAShowerFit` in reconstructing the position of electron (5.3a), muon (5.3b) and τ (5.3c) Neutral Current showers, and electron Charged Current showers (5.3d). Shown is the deviation between the reconstructed position and the neutrino vertex position. The histogram entries are shown as a color map, and the 16%, 50% and 84% quantiles are drawn on top.

by the nature of the Neutral current shower, where part of the energy is carried away by the undetected neutrino. The performance of `AAShowerFit` on the τ Charged current showers is in between these two scenarios. There is a bigger spread in the energy reconstruction performance than we see for the electron showers over the whole range of simulated energies. Especially striking is the lowest (18%) quantile, which is at -1 for most of the energy range. This means that the reconstruction of the energy failed and energy was reconstructed to be zero. This effect is caused by low energy τ decay showers, where either the τ lepton had a low energy or much energy was carried away by neutrinos produced in the τ decay. This results in a low number of hits, which causes the energy reconstruction to break down. Furthermore, the τ lepton can fly out of the detector, taking away an arbitrary amount of energy and therfore hits, so that there are even less hits available to perform the energy reconstruction.

At very high energies ($>1 \times 10^{6.5}$ GeV) the energy is underestimated

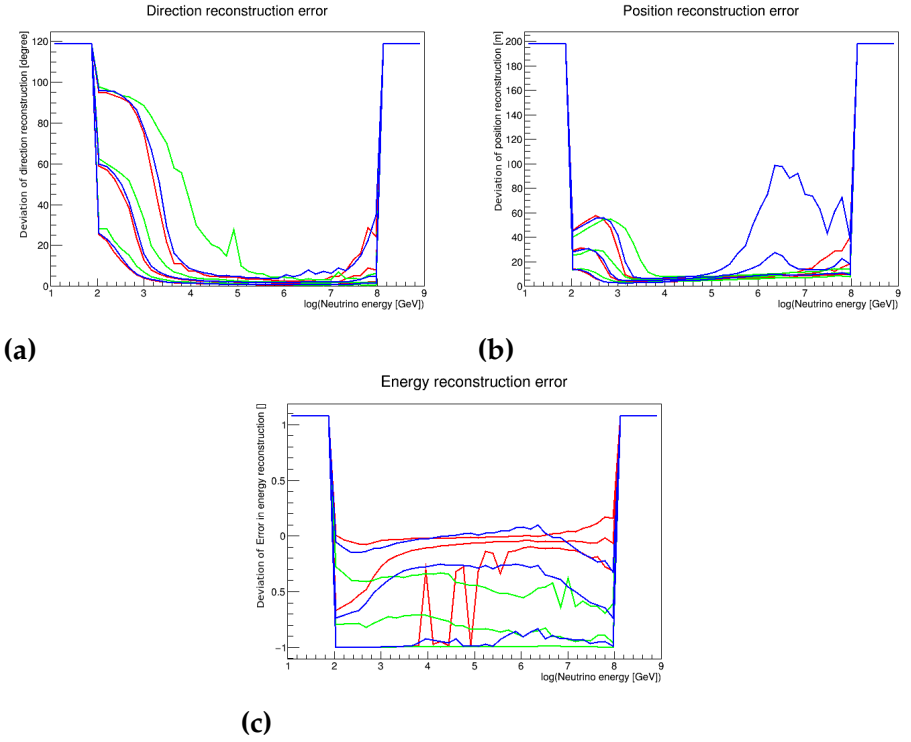

Figure 5.4: Performance of `AAShowerFit` in reconstructing the vertex direction (a), position (b) and energy (c) of τ Charged Current events (blue) compared to electron Charged Current events (red) and muon Neutral Current events (green). Shown are the deviation in direction and position and the fractional deviation in energy, as compared to the neutrino direction, vertex position and energy. The 16%, 50% and 84% quantiles are shown for all events.

for most of the events. This may be caused by the long travel length of the τ lepton, causing the second vertex, where the τ lepton decays, to occur outside of the detector volume. This is possible since the containment requirement only requires the neutrino vertex to be within the detector volume. The energy from the second, hadronic, shower is therefore not registered by the detector and is not taken into account by the reconstruction. This effect is also seen for the muon showers, where we know that part of the energy is not recorded by the detector.

Since the position reconstruction is most prominently affected by the travel length of the τ lepton, it is interesting to look further into the position reconstruction. The average travel length of the τ lepton increases with increasing energy due to relativistic effects. A τ lepton with an energy of 1 PeV has an average travel length of 50 m. The travel length of the τ lepton from the Monte Carlo information can be used to look directly at how the

travel length of the τ lepton affects the position reconstruction. This is shown in Figure 5.5. Here, the deviation of the position reconstruction is shown with respect to the neutrino vertex and with respect to the τ decay vertex.

In both plots, we see two highly populated lines, one around a position reconstruction deviation of zero, another around position reconstruction deviations equal to the τ travel length. This is a clear indication that, for almost all events, one of the two vertices positions is correctly reconstructed. The second interesting feature in these plots is the position of the quantiles. Comparing both plots, we see that the median follows the line of events reconstructed to be at the τ vertex in both cases, indicating that half of the events is reconstructed closer than the τ travel length to the neutrino vertex and that at least half of the events is reconstructed at the τ vertex. Together, these two observations indicate that over half of the events are reconstructed at the τ decay vertex. We therefore conclude that `AAShowerFit` is slightly biased to the τ decay vertex for its position reconstruction.

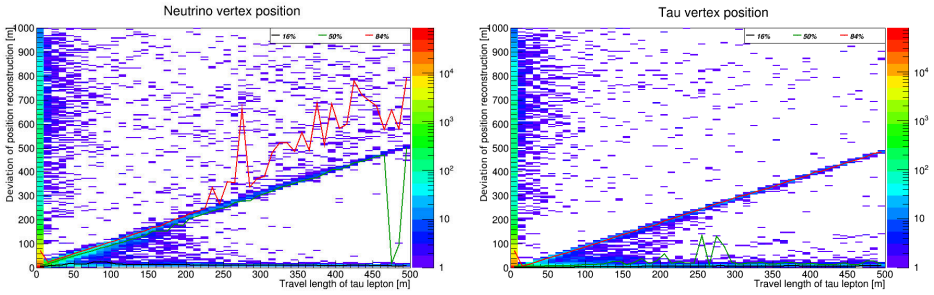

Figure 5.5: Performance of `AAShowerFit` in reconstructing the first (left) and second (right) vertex position of Charged Current τ to shower events, plotted against τ travel length.

5.2 Separate Showers

Using the Monte Carlo truth information, the hits in each event could be split into two sets: one set contains the hits coming from the neutrino shower, and the other set contains the other hits, which will therefore come from the τ shower. In this process, only the Monte Carlo hits could be used, because they have information on which particle created the hit, so there is no background and no simulated detector response in these split events.

Using these events, we can look at the reasons for `AAShowerFit` to be biased towards the second vertex as well as at the reconstruction perfor-

mance of `AAShowerFit` for both showers in an event separately; if we are to split the showers in a real event, how accurately would we be able to determine both shower positions?

5.2.1 Splitting

The two showers in each event are split according to the position at which the particle causing the hit is created. If this position is equal to the neutrino vertex, the hit goes into one file, otherwise, we conclude that the hit comes from a particle originating at the τ decay vertex and it is written to another file. After this process, we have two files, each containing only the hits coming from one of the two showers.

After the splitting, `AAShowerFit` is run on each of the two files separately. The performance of this reconstruction is shown in Figure 5.6. Since each file now only contains a single shower, we expect the performance of `AAShowerFit` to be comparable to what we saw for the Charged Current electron neutrino events. This is what we see in Figure 5.6. Therefore, the performance is better than the observed performance for the complete τ Double Bang events.

5.2.2 Reconstructing Separate Showers

For `AAShowerFit` to be able to reconstruct both showers of a double bang event, the showers have to be reconstructable one-by-one. Therefore, a containment requirement for both vertices to be in the active detector volume has been used (in the previous chapters, this containment requirement was only enforced on the reconstructed vertex). We looked at the percentage of events for which the position of both vertices was successfully reconstructed as a function of both energy and τ travel length. Successful reconstruction in this case has been defined as both vertices being reconstructed within a certain distance (in this evaluation 5, 10 and 20 m) from the simulated vertex. Figure 5.7 shows a plot showing the total number of events per bin, as well as the plots of the percentage of successful reconstructions for the three different criteria.

The percentage plots show that for events with low neutrino energy and τ travel length, only a small fraction of events have two reconstructable vertices. This is likely caused by the small number of hits in these low energy events and the small separation of the two showers, when the distance the τ lepton flies between showers is lower than 1×10^{-4} m, the travel length is not written to file, and the effective distance between the

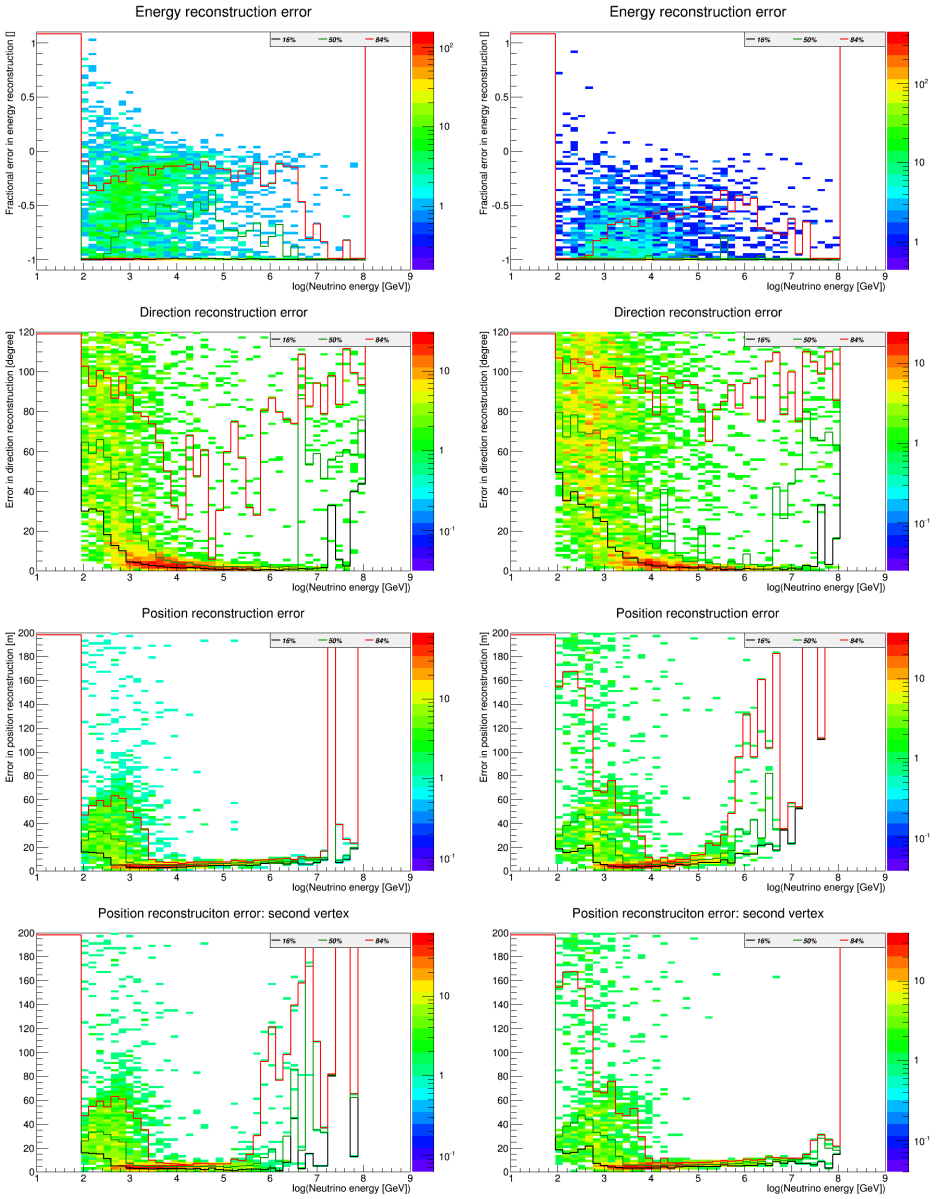

Figure 5.6: Performance of `AAShowerFit` one one τ neutrino Charged Current to shower file split according to the origin of the particles producing the hits. Hits from the first vertex are in the first file (the graphs on the left) and all other hits are stored in a second file (graphs on the right).

showers is recorded as zero. This makes it impossible to split the two showers in these low energy events.

For energies higher than 1×10^5 GeV, we see that the ratio of events where both vertices were successfully reconstructed is over 80% for dis-

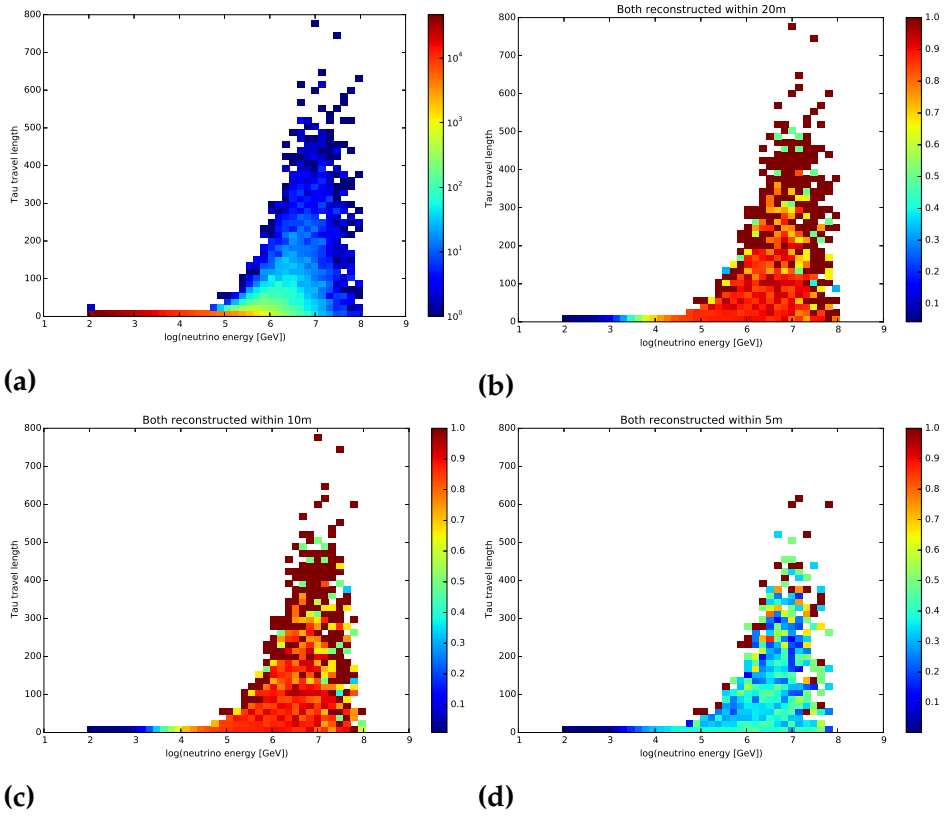

Figure 5.7: The investigation of the percentage of events for which a successful reconstruction of both vertices was achieved as a function of neutrino energy and τ travel length. (a) shows the total number of doubly contained events in each bin. (b), (c) and (d) show the fraction of events where both of the showers have been reconstructed within 20, 10 and 5 m respectively.

tances between the simulated and reconstructed vertex lower than 10 or 20 m. Here, there are many more hits and the τ lepton flies long enough for its travel length to be written to file (the minimum travel length for this to happen is 1×10^{-4} m) thereby making the splitting of the two showers possible. In most of the cases, this apparently leaves enough hits for both showers when split, independent of the energy distribution between the showers. As the τ travel length increases, we see that the fraction of successfully reconstructed events increases. This is mainly caused by the limited statistics in the bins. From these plots we can therefore only conclude that the probability to reconstruct both vertices after splitting is higher for events with higher neutrino energy. The effect of the τ travel length seems to be that the probability to reconstruct both vertices well

also increases, since the travel length is a measure for the τ leptons energy, but the statistics in the relevant areas Figure 5.7 are not high enough to conclude this.

Comparing Figure 5.7b, Figure 5.7c and Figure 5.7d, we see that the fraction of successful reconstructions is almost constant when we compare the plots for accuracies of 10 m and 20 m. For an accuracy of 5 m, we see a significant decrease in the fraction of successful reconstructions for energies above 1×10^4 GeV. This is caused by the fact that `AAShowerFit` reconstructs the shower maximum, which is, for these energies, about 5 m away from the shower vertex. We can use this result as a measure of the accuracy of `AAShowerFit` to reconstruct these split showers, showing that its position accuracy for these events is around 10 m for most events.

For real events, we would have no prior information on the positions of the two showers, so the containment requirement used here will not be applicable. Figure 5.8 shows the effect of this Monte Carlo information based containment requirement. Here, we see the fraction of events where both showers were reconstructed within 10 m from the true vertex in four cases: no containment requirement, a containment requirement on only the τ decay vertex, a containment requirement on the neutrino vertex and a containment requirement on both vertices (as was the case in Figure 5.7. Figure 5.9 shows the number of events per bin for these four cases.

In these figures, we see that, when there is no containment requirement, only a small fraction of the events could be correctly reconstructed. This is most likely due to the great amount of total events available, as we see in Figure 5.9d. The ratio of successful reconstructions of both vertices increases greatly when a containment requirement on one of the two vertices is imposed and is the highest for a containment requirement on both vertices. Reconstructing the two showers as one vertex and using that position for the containment requirement, as we have done in the rest of the analysis in this report, will probably result in ratios comparable to Figure 5.8b and Figure 5.8c, where a containment on one of the two Monte Carlo vertices was imposed. As we see in Figure 5.9, this greatly decreases the total number of available events in the higher energy and τ travel length regions.

When we compare Figure 5.9b and Figure 5.9c to Figure 5.9d, we see that there are less events at higher travel lengths that survive the double containment requirement. This is caused by the limited volume within both vertices have to be contained. This effect causes the low number of filled bins in Figure 5.8d. However, all of the filled bins in this plot have a high ratio, indicating that the containment requirement mainly selects events where a reconstruction of both vertices is possible. For low energies,

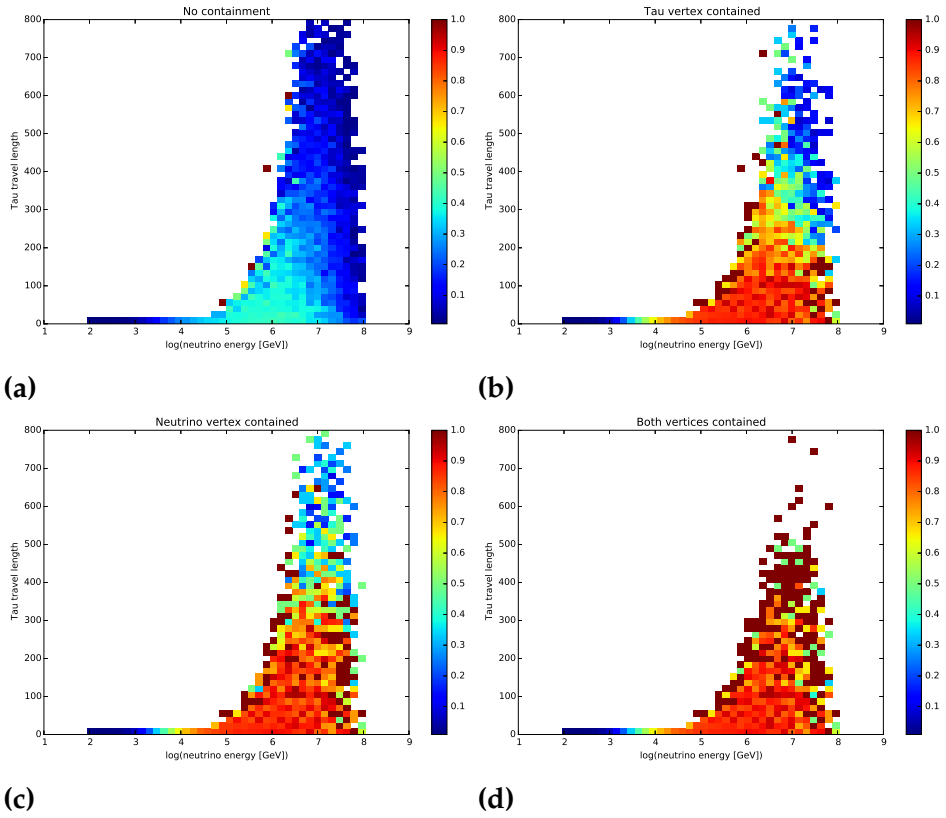

Figure 5.8: The fraction of events for which both vertices were reconstructed within 10 m from the true vertex for four cases: no containment requirement (a), τ decay vertex containment requirement (b), neutrino vertex containment requirement (c) and a containment requirement on both vertices (d).

the ratios are the same, but at higher energies and travel lengths, we see differences between the plots where only one vertex is contained and the plot where both are contained. The ratio of successful reconstruction is higher in this area when both vertices are contained, but, as we saw in Figure 5.7a, the statistics there are very low.

For energies above 1×10^7 GeV, we see that, for long τ travel lengths, the ratio of successful reconstructions for the τ containment is lower than that for the neutrino containment. Comparing Figure 5.9b and Figure 5.9c, we see that there are more events in this region that survive the τ decay vertex containment requirement than the neutrino vertex containment requirement. This might lead to the difference in the reconstruction ratios because the total number of events increases while the number of reconstructable events, which are mainly the events where both vertices are

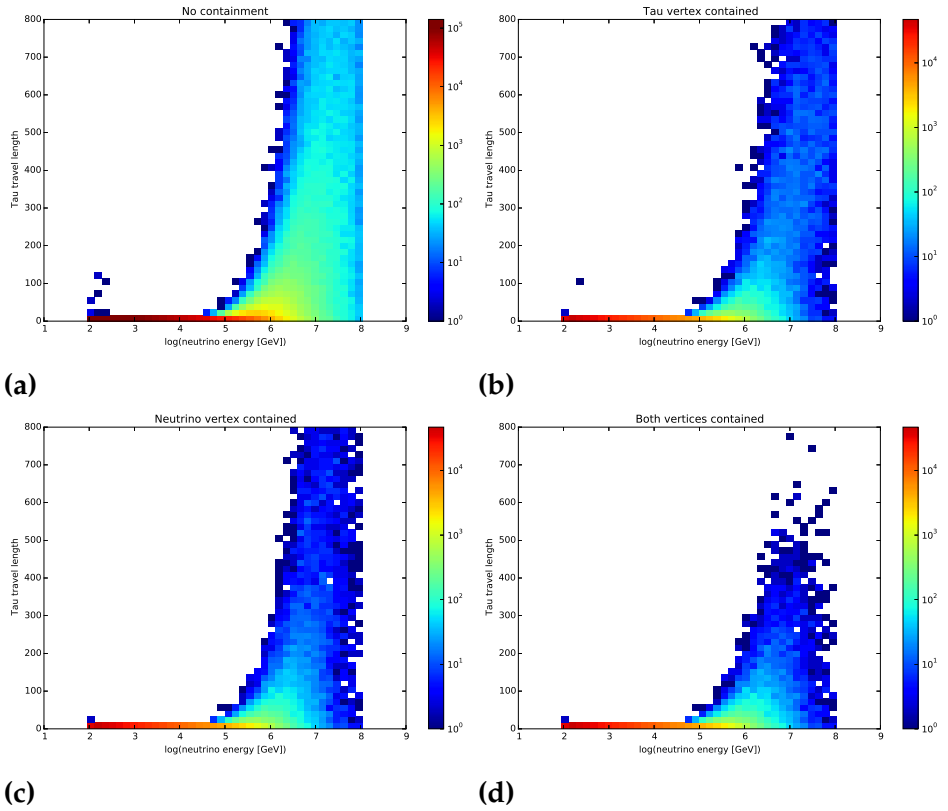

Figure 5.9: The number of evaluated events for the evaluation of the separate shower reconstruction in four cases: no containment requirement (a), τ decay vertex containment requirement (b), neutrino vertex containment requirement (c) and a containment requirement on both vertices (d).

contained, stays approximately the same.

In general, we can say that the containment requirement used greatly affects the number of events available for reconstruction. As we can see in Figure 5.9, especially the events at high energies and τ travel lengths suffer from the containment requirements due to the higher chance that one of the showers occur outside of the containment volume. Around 1×10^8 GeV, this decrease in the number of events is close to a factor of ten for the full length range.

5.2.3 Hit Distribution

Using the split files, we can look at the hit distribution between the two showers. The slight preference of `AAShowerFit` to reconstruct the position of the shower at the τ decay vertex could be explained if there are more

hits originating from this vertex. To investigate this, Figure 5.10 shows the number of hits in an event created by the neutrino shower as a fraction of the total number of hits in that event. This is shown for four ranges of τ travel length: 0-2.5 m, 2.5-20 m, 20-100 m and travel lengths above 100 m. For this plot, 1×10^9 events were processed and a containment requirement on both vertices was used.

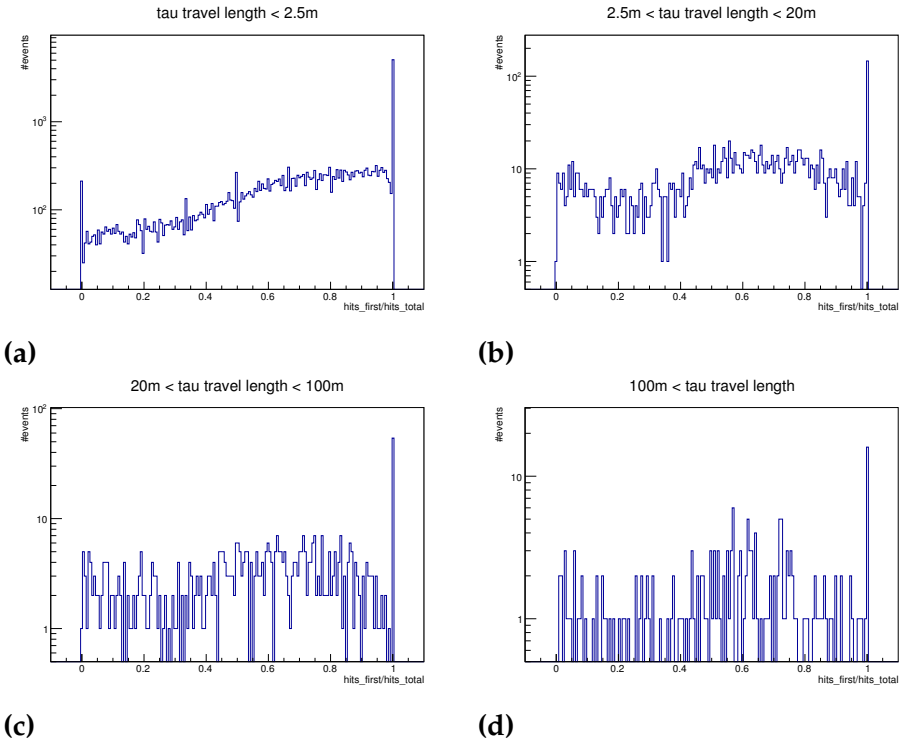

Figure 5.10: The fraction of hits originating at the neutrino vertex compared to the total number of hits in an event plotted for four ranges of τ travel length: 0 to 2.5 m(a), 2.5 to 20 m(b), 20 to 100 m(c) and travel lengths larger than 100 m(d)

In Figure 5.10a, we see two distinct peaks; at a fraction of 0 and a fraction of 1. These peaks indicate that all hits originated at exactly one vertex. If the τ lepton has a low energy, it could be possible that it's travel length is recorded in the data as zero. This happens when this flight path is under 1×10^{-4} m. In that case, the distinction between the two vertices would be impossible to make, resulting in all hits of the event coming from one of the two vertices. The peak at a ratio of one however, cannot be fully explained in this manner since it persists for higher travel lengths. Most likely, the reason for this is again a low energy τ lepton, which would cause a small shower and thus little or no hits. Another possible reason for this is that, as

was discovered after this research was done, the τ lepton does not decay in some of the simulated events. This is a flaw in the Monte Carlo productions that has been fixed since.

Besides the two peaks in Figure 5.10a, we see that, for these low travel lengths, there is an increasing trend in the number of events when we go towards all hits originating from the neutrino vertex. This can again be explained by the τ shower energy being lower than the neutrino shower energy and thus producing a smaller shower. When we look at the other three plots, we see that for these higher travel lengths the increasing trend is less visible, indicating that for these travel lengths the hit distribution between the two showers becomes more even.

From the plots in Figure 5.10, we do not get an indication why `AAShowerFit` would have a slight preference for the τ decay vertex. We observe that for events with τ travel lengths above 2.5 m is almost even, and that at lower travel lengths the neutrino vertex even produces more hits. If anything, this would cause a preference for the neutrino shower.

Since the reason to prefer the τ decay vertex cannot be found in the number of simulated hits in each of the showers, it might be caused by the hit selection of `AAShowerFit` . For the position reconstruction, the starting parameters of `AAShowerFit` are set to the DOM with the highest multiplicity. From this position, the hit selection for the M-estimator position fit is made. To see if there is a bias in this selection, the distance between the DOM with the highest multiplicity and the neutrino vertex is plotted against the distance of that DOM to the τ decay vertex. Figure 5.11 shows this plot for four different τ travel length ranges.

In Figure 5.11a, we see that for these short travel lengths the chosen DOM is equally distant from both vertices. This was expected because the separation of the showers is minimal. We also observe that for these events, the distance between the chosen DOM and the two vertices often greatly exceeds the distance between the vertices, indicating that the initial position used by the M-estimator fit is far from the actual showers. This is reflected in the low reconstruction performance for low energy events we saw before. This large deviation is again most likely caused by the low amount of hits that are recorded for these low energy showers.

Looking at Figure 5.11b, we see that the largest deviations are no longer present for these τ travel lengths, although the distance from both vertices still exceeds the τ travel length. For many events, we also see a slight bias in the initial position choice for the τ decay vertex, indicated by the points just above the diagonal. This bias becomes more prominent for longer τ travel lengths, as we see in Figure 5.11c.

For τ travel lengths exceeding 100 m, the bias for the τ decay vertex

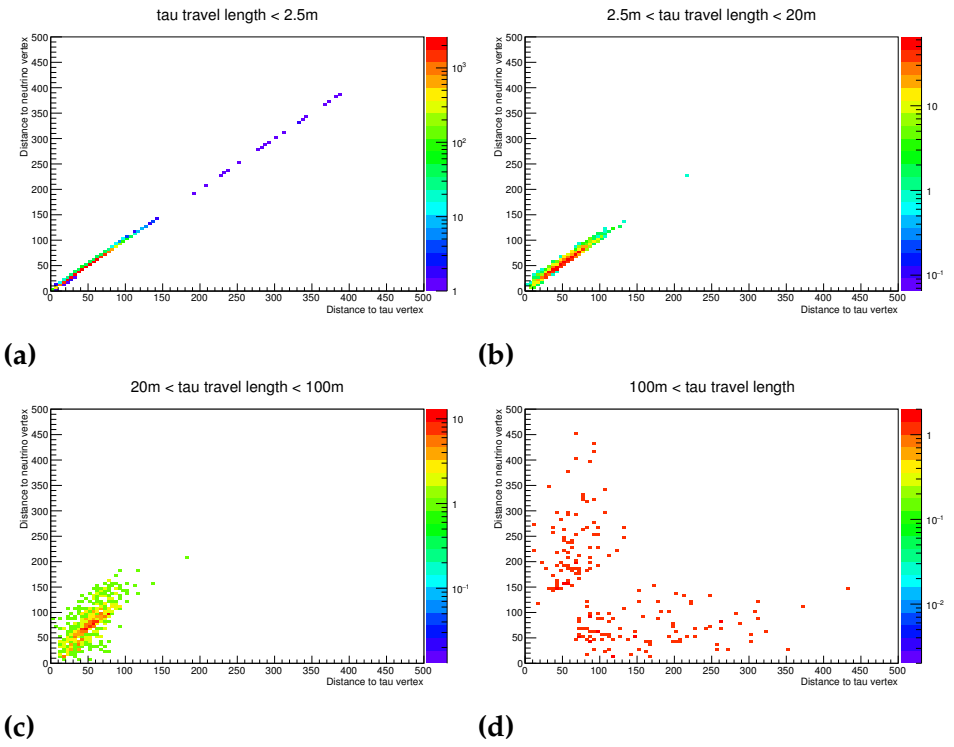

Figure 5.11: The distance from the PMT selected based on highest multiplicity to the neutrino and τ vertices shown for three different τ travel length ranges: 0 to 2.5 m(a), 2.5 to 20 m(b), 20 to 100 m(c) and travel lengths larger than 100 m(d).

seems to have disappeared and the points that are chosen are closer than the shower separation to one of the two vertices for most events. The statistics in this plot are however insufficient to conclude what the effect of this is on the bias.

From our investigation into the initial choice of position, based on the DOM with the highest multiplicity, we have seen a bias towards the τ decay vertex for events with τ travel lengths between 2.5 m and 100 m. This is most likely caused by the fact that the neutrino shower is directed along the τ travel path, thus causing an overlap between the two showers. This overlap causes the DOMs between the two showers to record the most hits.

Based on the position estimate from the DOM with the highest multiplicity, all hits that occur within 800 ns from the hit recorded on this DOM are selected for the M-estimator fit. Since we see a bias in the initial position selection, we might expect that the hits that are selected for the M-estimator fit will also show this bias and thereby explain the slight bias we see in the reconstructions by `AAShowerFit` . To investigate this, plots showing

the fraction of hits coming from the neutrino vertex to the total number of selected hits were made for four different τ travel lengths. These are shown in Figure 5.12.

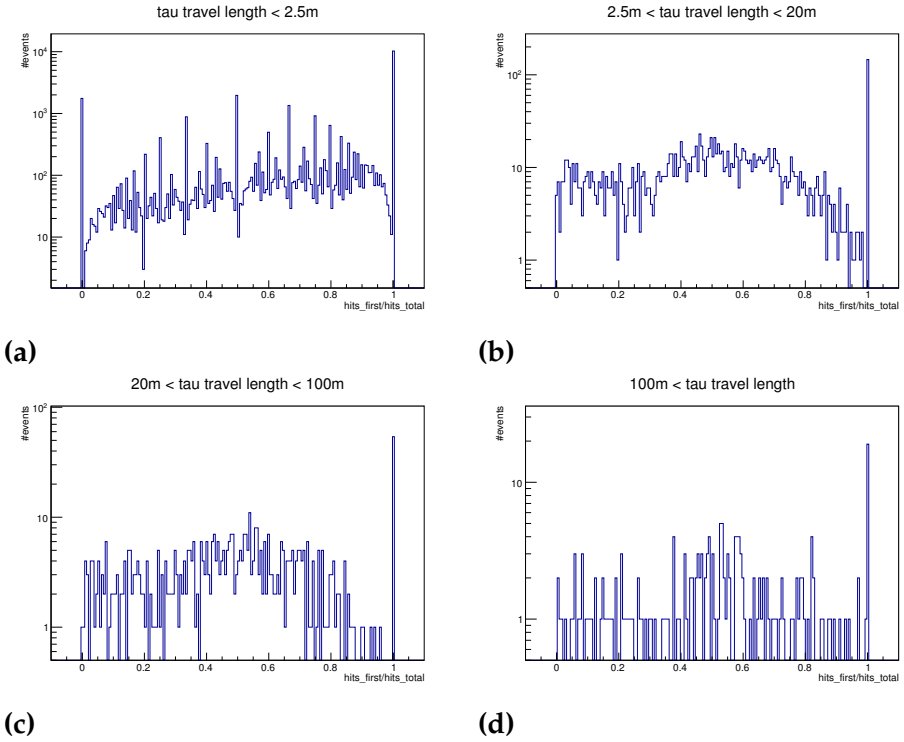

Figure 5.12: The fraction of hits selected for the position reconstruction originating from the neutrino vertex compared to the total number of hits selected for this reconstruction plotted for four ranges of τ travel length: 0 to 2.5 m(a), 2.5 to 20 m(b), 20 to 100 m(c) and travel lengths larger than 100 m(d).

Looking at Figure 5.12a, we see that both peaks at zero and one are still visible, but that the peak at zero, indicating that all hits originated at the τ decay vertex, has increased in size with respect to the peak at one. We also see that the increasing trend has diminished compared to what we observed for the raw hits. For the longer distances, we still see an approximately flat distribution. There is a slight shift in this distribution however. The broad hump we see around a fraction of 0.65 in Figure 5.10b has shifted to around 0.5 in Figure 5.12b, indicating that a larger fraction of the selected hits comes from the τ decay vertex than in the raw hits. This effect is also slightly visible in Figure 5.12c and Figure 5.12d, but the statistics there are too low to conclude this.

The selected hits for the M-estimator are, in general, closer to the τ decay

vertex than the raw hits. This was to be expected because the position and time on which these hits are selected was also slightly biased, as we see in Figure 5.11. This effect is small, but might explain the observed bias for the τ decay vertex in the position fit.

5.3 τ Identification

This last part of the results section will discuss how it is possible to identify τ Double Bang events based on the results we get from `AAShowerFit`. For this, some of the variables that are returned by the reconstruction are used: the reconstructed energy, the likelihood of the fit and the error in the reconstructed direction. The likelihood and error in direction are quality parameters of the reconstruction algorithm, by looking at their correlation with the reconstructed event energy, we might be able to distinguish τ events from electron events. The fit quality could be worse for double shower events, because there are hits from a second shower in the event. There is a low likelihood that these hits are caused by a shower at the reconstructed vertex, and since the likelihood estimator bases the likelihood value on all hits in the event, this should lower the overall likelihood value for events with two showers.

The likelihood is calculated by the energy and direction fit in the reconstruction algorithm of `AAShowerFit` . This step minimizes the likelihood function described in Equation 4.4. The minimal value found by this reconstruction step is stored as the likelihood of the fit. The angular error is determined using the matrix of statistical errors, which is also calculated by `AAShowerFit` . It describes the statistical error on the direction reconstruction. The likelihood and the angular error have been chosen because they do not require Monte Carlo information to be calculated.

Figure 5.13 shows the dependence of the likelihood and angular error of the fit on the reconstructed energy for both τ and electron Charged Current events. Here we can see that there is a slightly bigger spread in the likelihood of τ events for high energy events. Between the plots of the angular error, we see very little difference between the electron and τ neutrino events. The small differences we see here are probably caused by the large number of short travel length events that are also included in these plots.

In Figure 5.14a, the plot of likelihood versus reconstructed energy is shown for long- and short τ travel lengths separately. This plot shows little difference between the spread in likelihood for long- and short τ travel lengths although there seems to be a slight shift of the curve to lower

energies for the events with longer τ travel length.

In Figure 5.14b, the angular error versus the reconstructed energy is shown for the same two ranges of τ travel length. Here, we also see little difference between the short and long travel lengths. The sharp peaks at low energies and energies above 10×10^8 GeV for long travel lengths can be explained by the low number of events in these ranges. We see that in Figure 5.14 there are events with τ travel lengths above 50 m for energies below 1×10^5 GeV, where there are none in Figure 5.9. This is caused by badly reconstructed events. In Figure 5.14, the reconstructed energy is used in stead of the MC neutrino energy. If the energy in an event is badly reconstructed, the events might show up lower on the energy scale if the reconstructed energy is used. Se see that these events, for which the energy reconstruction was bad, generally have a higher likelihood value than correctly reconstructed events in that energy region and that their angular error is systematically lower.

The plots in Figure 5.14 show that there are small differences to be seen in the likelihood and angular error between τ events with short and long τ travel lengths, most prominently in the region where the reconstructed energy is small. Other parameters might show this difference more clearly. More investigation will be needed to find the right parameters to distinguish τ double bang events from single shower events.

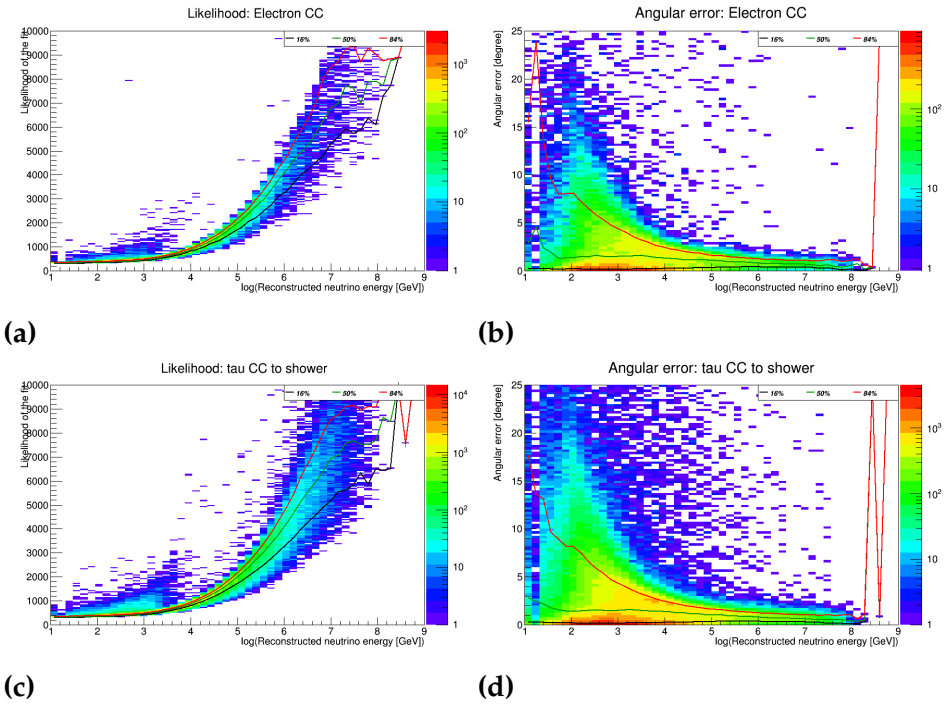

(a) **(b)**

(c) **(d)**

Figure 5.13: The dependence of the fit likelihood and angular error on the reconstructed energy for electron (5.13a and 5.13b) and τ (5.13c and 5.13d) Charged Current showers.

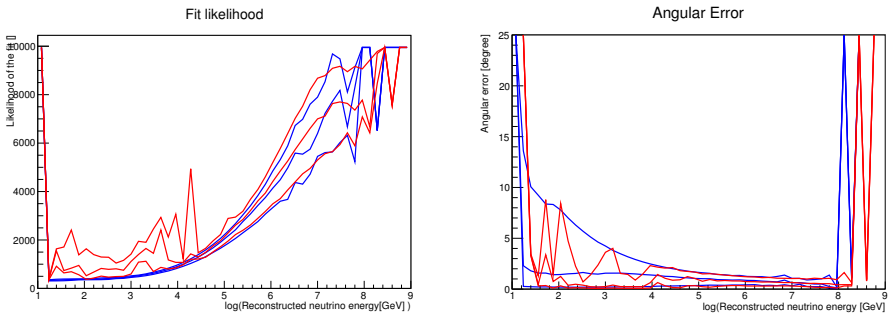

(a) **(b)**

Figure 5.14: The dependence of the fit likelihood (a) and angular error (b) on the reconstructed energy for τ Charged Current showers. Shown are plots for travel lengths between 0 and 20 m (blue) and between 50 and 1000 m (red).

Chapter 6

Conclusion

In this report, the possibilities to reconstruct and identify τ neutrino double shower events in the KM3NeT detector using `AAShowerFit` have been investigated. For the identification of these neutrinos, the Double Bang signature has been chosen, where a τ neutrino interacts with a proton, creating a shower and a τ lepton, which travels some distance before creating a second shower. The unique signature of this decay path, with two showers, makes it possible to distinguish it from other events through the reconstruction of the showers. Because `AAShowerFit` fits the entire event using a single shower hypothesis, we expect to see differences between the performance of this algorithm on Double Bang events and single shower events.

We have shown that `AAShowerFit` is accurate in determining the direction of the incoming τ neutrino in these events throughout the energy range, but that, for large energies, its accuracy in reconstructing the position decreases. This is caused by the travel length of the τ lepton, which increases with τ lepton energy. This separates the two showers, causing the single shower approximation of `AAShowerFit` to fail. When this happens, we observe that `AAShowerFit` still reconstructs one of the two vertices accurately. This effect can be used to separate the two showers and use a second shower reconstruction step to gain more information on the τ neutrino event.

From analyzing the reconstruction performance on these events with large τ travel length, we have identified a preference of `AAShowerFit` to reconstruct the τ decay vertex of the event. We have found a possible explanation for this in the selection of hits which is used for the position reconstruction. This selection is done based on the DOM with the highest multiplicity, showing that the event produces the most light close to the τ

decay vertex.

The spatial separation of the two showers was used to separate the hits from a Double Bang event into two separate files using Monte Carlo information. By looking at the reconstruction performance of `AAShowerFit` on these separate files we have seen that it is possible to successfully reconstruct both vertices in an event for energies higher than 10×10^5 GeV. When both vertices are contained in the detector this reconstruction was sucessfull for up to 80 % of the events. An investigation on how well this holds for different containment requirements indicates that this effect will remain in real events where we have no certain information on the position of the vertices, as long as some selection on the hits, based on a containment requirement, is used. A method to split the two showers according to the reconstructed vertex without using Monte Carlo data will also have to be developed in order to apply this reconstruction method on real data.

The specific characteristics of the τ double bang events could also be used to identify them. By looking at the output parameters of `AAShowerFit` , such as the angular error, the likelihood of the fit and the reconstructed energy, τ events might be distinguished from single shower events. In this report, investigating the relation of the reconstructed energy and the fit likelihood has shown fist differences in the signatures, but further investigation is needed to identify the most relevant parameters.

After this research, it was found that the simulated τ Double Bang data was flawed. The travel time of the τ lepton was not taken into account for its time information and consequently not in the hit time information, causing an offset that increases for longer τ travel length. The first reconstructions done on corrected data have shown that this only has little effect on the position reconstruction, and the direction and energy reconstruction do not rely on the time information. This means that the conclusions in this report should still be valid, although they will have to be checked with correct data.

Acknowledgements

This research was made possible by financial support from the Dutch Association for Scientific Research (NWO) and the Foundation for Fundamental Research of Matter (FOM).

References

[1] A. Heijboer, *Shower Direction Reconstruction: aashowerfit*, ANTARES-KM3NeT Internal Note, 2014.

[2] C. F. Cowen, *Tau neutrinos in IceCube*, Journal of Physics: Conference Series **60**, 227 (2007).

[3] K. Olive et al., *Review of Particle Physics*, Chin.Phys. **C38**, 090001 (2014).

[4] T. Kajita, *Atmospheric neutrino results from Super-Kamiokande and Kamiokande — Evidence for ν_μ oscillations*, Nuclear Physics B - Proceedings Supplements **77**, 123 (1999).

[5] D. Griffiths, *Introduction to Elementary Particles*, Physics textbook, Wiley, 2008.

[6] KM3NeT Collaboration, *KM3NeT: Conceptual Design for a Deep-Sea Research Infrastructure Incorporating a Very Large Volume Neutrino Telescope in the Mediterranean Sea*, Technical report, KM3NeT Collaboration, 2008.

[7] KM3NeT Collaboration, *KM3NeT: Technical Design for a Deep-Sea Research Infrastructure Incorporating a Very Large Volume Neutrino Telescope in the Mediterranean Sea*, Technical report, KM3NeT Collaboration, 2008.

[8] A. Margiotta, *Status of the KM3NeT project*, Journal of Instrumentation **9**, C04020 (2014).

[9] U. F. Katz, *The ORCA Option for KM3NeT*, Proceedings of the 15th International Workshop on Neutrino Telescopes (2013).

[10] P. A. Čerenkov, *Visible Radiation Produced by Electrons Moving in a Medium with Velocities Exceeding that of Light*, Phys. Rev. **52**, 378 (1937).

[11] KM3NeT Collaboration, *KM3NeT Strategy Document*, `http://www.km3net.org/publications/2014/KM3NeT-Strategy.pdf`, 2014.

[12] C. Kopper, *Performance studies for the KM3NeT Neutrino Telescope*, Nuclear Instruments and Methods in Physics Research Section A: Accelerators, Spectrometers, Detectors and Associated Equipment **692**, 188 (2012), 3rd Roma International Conference on Astroparticle Physics.

[13] ANTARES Collaboration, *GENHEN, Collaboration Wiki*, `http://www.antares.in2p3.fr`.

[14] ANTARES Collaboration, *The KM3 Package, Collaboration Wiki*, `http://antares.in2p3.fr`.

[15] KM3NeT Collaboration, *JPP, Collaboration Wiki*, `http://www.km3net.org`.